AD-A253 268

(2)

AD

Reports Control Symbol
OSD - 1366

TR-0313

SURFACE WIND SPEED DISTRIBUTIONS

June 1992

DTIC
ELECTE
JUL 3 0 1992
S A D

Elton P. Avara
Bruce T. Miers

92-20415

TECHNOLOGY TO WIN

US ARMY
LABORATORY COMMAND

ATMOSPHERIC SCIENCES LABORATORY
White Sands Missile Range, NM 88002-5501

92 7 28 063

NOTICES

Disclaimers

Destruction Notice

REPORT DOCUMENTATION PAGE

Form Approved
OMB No. 0704-0188

1. AGENCY USE ONLY *(Leave blank)*

2. REPORT DATE June 1992

3. REPORT TYPE AND DATES COVERED Final

4. TITLE AND SUBTITLE
Surface Wind Speed Distributions

5. FUNDING NUMBERS
TA: 62784/AH71/E

6. AUTHOR(S)
Elton P. Avara and Bruce T. Miers

7. PERFORMING ORGANIZATION NAME(S) AND ADDRESS(ES)
U.S. Army Atmospheric Sciences Laboratory
White Sands Missile Range, NM 88002-5501

8. PERFORMING ORGANIZATION REPORT NUMBER
ASL-TR-0313

9. SPONSORING/MONITORING AGENCY NAME(S) AND ADDRESS(ES)
U.S. Army Laboratcry Command
Adelphi, MD 20783-1145

10. SPONSORING/MONITORING AGENCY REPORT NUMBER

11. SUPPLEMENTARY NOTES

12a. DISTRIBUTION/AVAILABILITY STATEMENT
Approved for public release; distribution is unlimited.

12b. DISTRIBUTION CODE

13. ABSTRACT *(Maximum 200 words)*

Some weapon systems are sensitive to winds in the lowest layers of the atmosphere. Wind speed distributions and random wind speeds derived from the distributions are often required to help determine the operational capabilities of these systems. A literature survey revealed investigators usually used either a log-normal or a Weibull distribution as the model for the distribution of wind speeds independent of direction. In addition to these two distributions, a gamma distribution is also evaluated in this report. Wind speeds observed in three different geographical regions during nine selected meteorological conditions (weather classes), three diurnal time periods, and five seasonal time periods were evaluated. This report contains the results of the wind speed analysis for some of the combinations of weather classes, diurnal time periods, and seasonal time periods for each of the three geographical regions--European Lowlands, European Highlands, and Mideast Desert. The observed wind speed distributions were adequately presented by the analytical distributions except in a few cases. For those exceptions, the observed empirical wind speed distributions should be used rather than the analytical distributions to generate random wind speeds in simulation studies.

14. SUBJECT TERMS
wind speed, distributions, Weibull
lognormal, gamma

15. NUMBER OF PAGES 67

16. PRICE CODE

17. SECURITY CLASSIFICATION OF REPORT	18. SECURITY CLASSIFICATION OF THIS PAGE	19. SECURITY CLASSIFICATION OF ABSTRACT	20. LIMITATION OF ABSTRACT
Unclassified	Unclassified	Unclassified	SAR

NSN 7540-01-280-5500

Standard Form 298 (Rev 2-89)
Prescribed by ANSI Std Z39-18
298-102

CONTENTS

LIST OF ILLUSTRATIONS

Tables

Figures

1. INTRODUCTION

The Program Manager (PM) for BAT (PM-BAT) and his associated contractors (CAS, Incorporated, and Dynetics, Incorporated) have a requirement to find analytical distributions to adequately represent the observed wind speed distributions obtained under different meteorological conditions, at different time periods, and at different geographical regions of the world. These distributions are required to test the operational capabilities of the BAT system. The U.S. Army Atmospheric Sciences Laboratory (ASL) was requested to perform the task.

Dramatic changes in the atmosphere occur each day on the average as the sun rises and sets. Because diurnal variations are most prominent in the atmosphere's lower layers, changes in boundary layer winds have been documented as well as for other atmospheric variables (Holton, 1967). Frequency of occurrence of low wind speeds has important applications in air pollution analysis or for nuclear-biological-chemical (NBC) predictions for military applications. The predictions of frequencies of high wind speeds also have important applications in the areas of structural design and assessment of potential output from wind powered generators.

Most wind speed data used in this analysis are from measurements made by rotary cup anemometers. For low wind speed measurements, two errors are inherent in using cup anemometers: static friction and dynamic friction. A starting wind speed must be sufficient to overcome static friction and cause the cups to turn. Dynamic friction becomes a factor as the wind decreases from a speed above the starting threshold until the cups stop turning. Higher wind speed measurements are also subject to an error known as overspeeding. Overspeeding occurs because the anemometer responds more quickly to an increase in speed than to a decrease in speed. In a turbulent wind field the mean value of the anemometer reading will be higher than the true mean. Also, an error caused by vertical wind fluctuations is of the same sign as the overspeeding error. The additive effect of these errors can cause measurements to be greater than the true wind speed by as much as 10 percent (Mage, 1980).

Investigators have examined various statistical models for wind speed frequency distributions that range from calm to the maximum observed wind speed. A Planck distribution was investigated by Dinkelacker (1949) and Wentink (1974). A Rayleigh distribution (a chi-square distribution with 2 degrees of freedom) has been used by Narovlyanskii (1968) and Baynes (1974). Crutcher and Baer (1962) showed that the bivariate normal distribution is adequate for most wind samples. The Pearson Type III (gamma) was used by Putnam (1948) and Sherlock (1951) to describe wind speed distributions. The Weibull distribution was used to fit both upper air data (Baynes and Davenport, 1975) and surface wind speed data (Wentink, 1976). Justus et al., (1976) were successful in fitting the Weibull distribution to data from 135 sites. The Weibull model has been an especially useful tool for wind power analysis (Hennessey, 1977). Stewart and Essenwanger (1978) examined the Weibull distribution, and Luna and Church (1974) examined the log-normal distribution as models for the distribution of wind speeds independent of direction.

2. CLIMATOLOGY DATA BASE AVAILABLE

The ASL maintains a climatology data base containing historical weather observations from more than 1000 locations in North, Central, and South America; Northern, Central, and Southern Europe; Mideast and North Africa; Southwest, Southern, and Southeast Asia; and Korea. These data were obtained over a period of years from the U.S. Air Force Environmental Technical Applications Center (USAFETAC) at Scott Air Force Base, Illinois. The period-of-record for the data from each station is generally 11 years or less and may be anywhere from 1966-76 to 1976-86, depending upon which year the data were obtained from the USAFETAC.

The regions of interest to the PM-BAT were the European Lowlands, the European Highlands, and the Mideast Desert geographical areas (Miers et al., 1985a; Miers et al., 1985b). The stations located in each of these regions are listed in tables 1 through 3. The period-of-record for the data from most of these stations is 1966-76.

For the two European regions, the PM-BAT was interested in winter and annual wind speed distributions obtained by grouping the observations from all hours of the day. Winter for these regions is defined to be November, December, January, and February. For the Mideast Desert region, the PM-BAT was interested in summer and annual wind speed distributions obtained by grouping the observations taken at night into one group and the observations taken during the daytime into another group. Summer for the Mideast Desert region is defined to be June, July, and August.

The 3-hourly observations (0000, 0300, ..., 2100 GMT) in the data base tend to be more reliable and consistent over time than the observations taken at the other hours of the day. Therefore, the 3-hourly observations were the only observations included in the analysis for any region, season, or period of the day.

3. WEATHER CLASSES

The PM-BAT was interested in the wind speed distributions derived from observations taken in different weather conditions or classes. A weather class is a specific configuration of cloud cover and cloud base height, visibility, and obscuration type. These observation weather classes were defined by representatives of the PM-BAT. The specific classes requested are defined in table 4 as WXCL-1 through WXCL-6, WXCL-8, and WXCL-9. The PM-BAT requested the wind speed information for WXCL-1 to WXCL-6 for the European regions and WXCL-1, WXCL-8, and WXCL-9 for the Mideast region. The class WXCL-7 was added by the authors for the European regions to allow the PM-BAT to see the results of fitting analytical distributions to wind speeds observed during fog conditions without regard to the type of fog.

TABLE 1. A LIST OF THE STATIONS LOCATED IN THE EUROPEAN LOWLANDS GEOGRAPHICAL REGION

STATION NUMBER	STATION NAME	LATITUDE (DEG:MIN)	LONGITUDE (DEG:MIN)	ELEVATION (METERS)
062400	AMSTERDAM/SCHIPHOL, NL	+52:18	-004:46	-0004
062700	LEEUWARDEN, NL	+53:13	-005:46	+0001
062750	DEELEN, NL	+52:04	-005:53	+0048
062900	TWENTHE/ENSCHED, NL	+52:16	-006:54	+0035
063100	VLISSINGEN, NL	+51:27	-003:36	+0010
063440	ROTTERDAM AIRPORT, NL	+51:57	-004:26	-0004
063500	GILZE-RIJEN, NL	+51:34	-004:56	+0013
063750	VOLKEL, NL	+51:39	-005:42	+0022
063800	ZUID-LIMBURG/MAAST., NL	+50:55	-005:46	+0114
064320	CHIEVRES, BX	+50:34	-003:50	+0060
064510	BRUSSELS INTL, BX	+50:54	-004:28	+0055
064560	FLORENNES, BX	+50:14	-004:39	+0284
064790	KLEIN-BROGEL, BX	+51:10	-005:28	+0060
070150	LILLE/LESQUIN, FR	+50:34	-003:06	+0048
070700	REIMS/CHAMPAGNE, FR	+49:18	-004:02	+0095
071690	ST. DIZIER/ROBINSON, FR	+48:38	-004:54	+0139
091700	WARNEMUNDE, DD	+54:11	-012:05	+0004
091850	GRIEFSWALD/WIECK, DD	+54:06	-013:27	+0002
093610	MAGDEBURG, DD	+52:06	-011:35	+0079
094880	DRESDEN/KLOTZCHE, DD	+51:08	-013:46	+0230
094920	COTTBUS, DD	+51:46	-014:18	+0068
095540	ERFURT/BINDERSLEBEN, DD	+50:59	-010:58	+0315
100260	HUSUM, FRG	+54:31	-009:09	+0028
100340	EGGEBEK/FLENSBURG, FRG	+54:38	-009:21	+0020
101290	BREMERHAVEN, FRG	+53:32	-008:35	+0007
101470	HAMBURG/FUHLSBUTTEL, FRG	+53:38	-009:59	+0016
102180	AHLHORN, FRG	+52:53	-008:14	+0049
102240	BREMEN, FRG	+53:03	-008:47	+0003
103130	MUNSTER, FRG	+51:58	-007:36	+0064
103140	HOPSTEN, FRG	+52:20	-007:33	+0039
103200	GUTERSLOH, FRG	+51:56	-008:19	+0070
103380	HANNOVER, FRG	+52:28	-009:42	+0055
103840	BERLIN/TEMPLEHOF, FRG	+52:28	-013:24	+0050
104000	DUSSELDORF, FRG	+51:17	-006:46	+0045
104020	WILDENRATH, FRG	+51:07	-006:13	+0089
123300	POZNAN/LAWICA, PL	+52:25	-016:50	+0092

TABLE 2. A LIST OF THE STATIONS LOCATED IN THE EUROPEAN HIGHLANDS GEOGRAPHICAL REGION

STATION NUMBER	STATION NAME	LATITUDE (DEG:MIN)	LONGITUDE (DEG:MIN)	ELEVATION (METERS)
065900	LUXEMBOURG/FINDEL, BX	+49:37	-006:13	+0491
071810	NANCY/OCHEY, FR	+48:35	-005:58	+0336
072920	LUXEUIL/ST. SAUVEUR, FR	+47:47	-006:21	+0278
095460	KALTENNORDHEIM, DD	+50:38	-010:09	+0487
095770	KARL-MARX-STADT, DD	+50:49	-012:54	+0357
104380	KASSEL, FRG	+51:19	-009:29	+0158
105020	NORVENICH, FRG	+50:50	-006:40	+0117
105445	FULDA AAF, FRG	+50:33	-009:39	+0305
106070	SPANGDAHLEM, FRG	+49:58	-006:42	+0365
106100	BITBURG, FRG	+49:57	-006:34	+0375
106130	BUCHEL/COCHEM, FRG	+50:10	-007:04	+0477
106140	RAMSTEIN, FRG	+49:26	-007:35	+0237
106160	HAHN, FRG	+49:57	-007:15	+0503
106590	KITZINGEN AAF, FRG	+49:45	-010:12	+0210
106870	GRAFENWOHR, FRG	+49:42	-011:57	+0414
107080	SAARBRUCKEN/ENSHEIM, FRG	+49:13	-007:07	+0322
107140	ZWEIBRUCKEN, FRG	+49:13	-007:25	+0343
107380	STUTTGART/ECHTER, FRG	+48:41	-009:12	+0396
107630	NURNBERG, FRG	+49:30	-011:05	+0319
108570	LANDSBERG/LECH, FRG	+48:04	-010:54	+0623
108580	FURSTENFELDBRUCK, FRG	+48:12	-011:16	+0518
108660	MUNCHEN/RIEM, FRG	+48:08	-011:43	+0529
110100	LINZ/HORSCHING, OS	+48:14	-014:11	+0297
111500	SALZBURG, OS	+47:48	-013:00	+0430
114060	CHEB, CZ	+50:05	-012:24	+0474
115180	PRAGUE/RUZYNE, CZ	+50:06	-014:17	+0380
125100	SNEIZKA, PL	+50:44	-015:44	+1603

TABLE 3. A LIST OF THE STATIONS LOCATED IN THE MIDEAST DESERT GEOGRAPHICAL REGION

STATION NUMBER	STATION NAME	LATITUDE (DEG:MIN)	LONGITUDE (DEG:MIN)	ELEVATION (METERS)
171700	VAN, TU	+38:27	-043:19	+1667
171950	KAYSERI/ERKILET, TU	+38:47	-035:29	+1052
172400	ISPARIA, TU	+37:45	-030:33	+0997
172800	DIYARBAKIR, TU	+37:54	-040:12	+0686
400070	ALEPPO/NEIRAB, SY	+36:11	-037:13	+0390
400160	HASSAKAH, SY	+36:30	-040:45	+0295
400390	RAQQA, SY	+35:56	-039:01	+0245
400610	PALMYRA/TUDMUR, SY	+34:33	-038:18	+0395
400800	DAMASCUS NEW INTL, SY	+33:25	-036:31	+0610
402600	HOTEL FIVE, TJ	+32:12	-037:08	+0668
402700	AMMAN/KING ABDULLAH, TJ	+31:59	-035:59	+0767
403100	MA'AN, TJ	+30:10	-035:47	+1069
403560	TURAIF/AL TURAYF, SD	+31:41	-038:40	+0827
403620	RAFHA, SD	+29:38	-043:29	+0443
403750	TABOUK, SD	+28:22	-036:35	+0771
403940	HAIL, SD	+27:31	-041:44	+0992
404300	MEDINA/AL MADINAH, SD	+24:33	-039:43	+0646
404380	RIYADH INTL, SD	+24:42	-046:44	+0624
406080	MOSUL/MOSSOUL, IQ	+36:19	-043:09	+0223
406340	HADITHA/HAQLANIYA, IQ	+34:04	-042:22	+0140
406420	RUTBAH, IQ	+33:02	-040:17	+0615
406500	BAGHDAD INT (ORBW), IQ	+33:14	-044:14	+0034
406740	SEMAWA, IQ	+31:18	-045:16	+0006
407060	TABRIZ, IR	+38:08	-046:15	+1367
407430	SABZEVAR, IR	+36:13	-057:40	+0941
407470	SANANDAJ, IR	+35:20	-047:00	+1538
407540	TEHRAN/MEHRABAD, IR	+35:41	-051:19	+1204
407910	TABAS, IR	+33:36	-056:54	+0691
408000	ESFAHAN, IR	+32:37	-051:40	+1598
408290	ZABUL, IR	+31:01	-061:29	+0487
408410	KERMAN, IR	+30:15	-056:58	+1748
408590	FASA, IR	+28:58	-053:41	+1382
408790	IRANSHAHR, IR	+27:12	-060:42	+0566
409110	MAZARI-SHARIF, AH	+36:42	-067:12	+0378
409130	KUNDUZ, AH	+36:40	-068:55	+0433
409380	HERAT, AH	+34:13	-062:13	+0964
409740	FARAH, AH	+32:22	-062:11	+0700
409860	ZARANJ/NIMROZE, AH	+31:06	-061:56	+0478
409900	KANDAHAR, AH	+31:30	-065:51	+1010
417100	NOKKUNDI, PK	+28:49	-062:45	+0679
417120	DALBANDIN, PK	+28:53	-064:24	+0848
417390	PANJGUR, PK	+26:58	-064:06	+0968
623060	MERSA MATRUH, UB	+31:20	-027:13	+0028
623180	ALEXANDRIA/NOUZHA, UB	+31:12	-029:57	-0003

Table 3. (cont)

STATION NUMBER	STATION NAME	LATITUDE (DEG:MIN)	LONGITUDE (DEG:MIN)	ELEVATION (METERS)
623330	PORT SAID/EL GAMIL, UB	+31:17	-032:14	+0003
623660	CAIRO INTL, UB	+30:08	-031:24	+0112
623870	EL MINYA/MINIA, UB	+28:05	-030:44	+0039
624140	ASWAN/ASWAN DAM, UB	+23:58	-032:47	+0200
624230	FARAFRA, UB	+27:03	-027:58	+0090
626500	DONGOLA, SU	+19:10	-030:29	+0226
627210	KHARTOUM, SU	+15:36	-032:33	+0382
627300	KASSALA, SU	+15:28	-036:24	+0500
627810	EN NAHUD, SU	+12:42	-028:26	+0565

TABLE 4. DEFINITIONS OF THE NINE OBSERVATION WEATHER CLASSES IN TERMS OF CLOUD COVER, CLOUD BASE HEIGHT, OBSCURATION TYPE, AND VISIBILITY

LABEL	DEFINITION
WXCL-1	No Clouds (no clouds or no clouds with bases <= 3000 m)
WXCL-2	Clouds with bases <= 3000 m
WXCL-3	Clouds with bases <= 3000 m and Precipitation
WXCL-4	Clouds with bases <= 3000 m and Advective Fog
WXCL-5	Clouds with bases <= 3000 m and Precipitation and Advective Fog
WXCL-6	Radiative Fog
WXCL-7	Fog
WXCL-8	Sandstorms and Dust
WXCL-9	Low Visibility (3 <= visibility <= 10 km)

By World Meteorological Organization (WMO) standards, a fog can be reported only when the visibility is not more than 1000 m. The PM-BAT wished to make a distinction between radiative and advective fog conditions. Observations in the ASL climatology data base do contain fog reports, but they do not contain information about the type of fog reported. To satisfy the requirements of the PM-BAT, definitions of radiative and advective fogs were taken from the USAFETAC electro-optical (EO) climatology software (USAFETAC, 1991). A reported fog was classified as radiative fog if the wind speed was less than 3.5 m/s (7 kn). Similarly, a reported fog was classified as advective fog if the wind speed was at least 3.5 m/s.

4. ANALYTICAL DISTRIBUTIONS

Three analytical distributions were selected for potential use in representing the observed wind speed distributions. They were chosen based upon the work of previous researchers referred to in section 1 and the request from the PM-BAT to specifically investigate the gamma distribution. These three candidate distributions were the gamma, log-normal, and Weibull. Each of these distributions performed reasonably well at representing the observed wind speed distributions for most of the weather classes.

The gamma probability distribution is defined by

$$f(x;\alpha,\beta) = \frac{(\frac{x}{\beta})^{(\alpha-1)}\exp[-(\frac{x}{\beta})]}{\beta\Gamma(\alpha)} \tag{1}$$

where $\Gamma(\alpha)$ is the gamma function with argument α, $x > 0$, $\alpha > 0$, and $\beta > 0$.

The log-normal probability distribution is defined by

$$f(x;\mu,\sigma) = \frac{\exp[-\frac{1}{2}(\frac{\ln(x)-\mu}{\sigma})^2]}{x\sigma\sqrt{2\pi}} \tag{2}$$

where μ is the expected value and σ is the standard deviation of $\ln(x)$ and $x > 0$.

The Weibull probability distribution is defined by

$$f(x;\alpha,\beta) = (\frac{\alpha}{\beta})(\frac{x}{\beta})^{\alpha-1}\exp[-(\frac{x}{\beta})^{\alpha}] \tag{3}$$

where $x > 0$, $\alpha > 0$, and $\beta > 0$.

In this report μ and β are called scale parameters because changing their values either tends to move the center or skew the distribution toward higher or lower values. σ and α are called shape parameters because changing their values tends to change the shape of the distribution to either a more peaked or a flatter form.

Three procedures for computing values for α and β or μ and σ were considered for fitting the analytical distributions to the observed wind speed distributions (histograms). These procedures are the method of moments, maximum likelihood, and nonlinear least squares fit to the observed cumulative probability distribution. For each observed wind speed distribution, the PM-BAT was interested in determining the best of the three analytical distributions and the associated parameter values. Once the name of the best analytical distribution and the distribution parameter values are known, the estimation of the tail probability of the wind speed is possible.

The "goodness-of-fit" of the analytical distributions was compared by computing both the mean absolute difference and the root-mean-square (rms) difference between the observed and each of the three analytical cumulative distributions. After thoroughly comparing the analytical distributions using both criteria, we decided to use the minimum rms difference to make the final selection.

When this criterion is used, the method of moments generally yields parameter estimates that do not perform as well as the other two procedures. The maximum likelihood procedure tends to yield better estimates of the parameters than the method of moments. The nonlinear least squares fit gives the best parameter estimates, as expected by the selection criterion.

4.1 Method of Moments

The expected value of x for the gamma distribution is given by

$$E[x] = \alpha\beta \tag{4}$$

and the variance of x is given by

$$VAR[x] = \alpha\beta^2 \ . \tag{5}$$

These two equations can be used to compute values of α and β for the gamma distribution using observed data to estimate E[x] by the mean value of the observed data and VAR[x] by the sample variance of the observed data giving

$$\beta = \frac{VAR[x]}{E[x]} \tag{6}$$

and

$$\alpha = \frac{E[x]}{\beta} \ . \tag{7}$$

This procedure for obtaining values for the distribution parameters is called the method of moments.

Using the method of moments to compute values for μ and σ in the log-normal distribution gives

$$\mu = E[\ln(x)] \tag{8}$$

and

$$\sigma = \sqrt{VAR[\ln(x)]} \quad , \tag{9}$$

where E[ln(x)] and VAR[ln(x)] are estimated from the data by using the mean value and sample variance of the natural logarithm of the wind speed data.

The advantage of using E[ln(x)] and VAR[ln(x)] rather than E[x] and VAR[x] to estimate μ and σ is quite obvious when one considers the relationship between the distribution parameters and E[x] and VAR[x] given by

$$E[x] = \exp[\mu + \frac{1}{2}\sigma^2] \tag{10}$$

and

$$VAR[x] = \exp(2\mu + \sigma^2)[\exp(\sigma^2) - 1] . \tag{11}$$

The expected value of x for the Weibull distribution is given by

$$E[x] = \frac{\beta}{\alpha}\Gamma(\frac{1}{\alpha}) \tag{12}$$

and the variance of x is given by

$$VAR[x] = \frac{\beta^2}{\alpha}[2\Gamma(\frac{2}{\alpha}) - \frac{1}{\alpha}[\Gamma(\frac{1}{\alpha})]^2] . \tag{13}$$

It is rather difficult to use the method of moments to compute values of α and β for the Weibull distribution using estimates of E[x] and VAR[x] obtained from observed data. Considering the computational time required to iteratively solve this system of equations and the general inferior quality of the parameter estimates, this procedure was not used to compute the Weibull distribution parameters.

4.2 Maximum Likelihood

The maximum likelihood procedure involves finding the parameter values that maximize the likelihood function of the distribution. For the gamma distribution these parameter values are obtained by iteratively solving the following system of equations:

$$\ln(\beta) + \Psi(\alpha) = E[\ln(x)] \tag{14}$$

$$\alpha\beta = E[x] \tag{15}$$

where $\Psi(\alpha)$ is the digamma function, $\ln[\Gamma(\alpha)]'$ (′ indicating first derivative with respect to α), with $\Gamma(\alpha)$ being the gamma function with argument α.

The maximum likelihood estimates of the log-normal distribution parameters are the same as those given in equations (8) and (9) by the method of moments.

The maximum likelihood estimates of the Weibull distribution parameters are obtained by iteratively solving the following system of equations.

$$\frac{E[x^{\alpha}\ln(x)]}{E[x^{\alpha}]} - \frac{1}{\alpha} = E[\ln(x)] \tag{16}$$

$$\beta = E[x^{\alpha}]^{\frac{1}{\alpha}} \ . \tag{17}$$

4.3 Nonlinear Least Squares Fit

The least squares fit was performed on observed cumulative distribution values $\{P_i,\ i = 1, 2, \ldots, N\}$ corresponding to discrete values of the wind speed, X, denoted by $\{X_i,\ i = 1, 2, \ldots, N\}$, where N is the number of wind speed intervals. Each wind speed interval had a width of 0.5 m/s. N was determined by choosing the first interval of the observed wind speed frequency of occurrence histogram such that all intervals greater than the Nth contained no occurrences of wind speed.

The three analytical distributions are clearly nonlinear with respect to the distribution parameters α, β, μ, and σ. To determine the least squares estimates of these parameter values, a procedure was used to linearize the distributions (at least in the neighborhood of any specific values of the parameters).

Consider the integral of the probability distribution given by

$$F(X;\alpha,\beta) = \int_0^X f(x;\alpha,\beta)\,dx \ . \tag{18}$$

By letting

$$\alpha = \alpha_0 + \delta\alpha \tag{19}$$

and

$$\beta = \beta_0 + \delta\beta \ , \tag{20}$$

equation (18) becomes

$$F(X;\alpha_0 + \delta\alpha, \beta_0 + \delta\beta) = \int_0^X f(x;\alpha_0 + \delta\alpha, \beta_0 + \delta\beta)\,dx \ . \tag{21}$$

To a first-order approximation using small values for $\delta\alpha$ and $\delta\beta$

$$F(X;\alpha,\beta) = F(X;\alpha_0,\beta_0) + \frac{\partial F(X;\alpha_0,\beta_0)}{\partial\alpha}\delta\alpha + \frac{\partial F(X;\alpha_0,\beta_0)}{\partial\beta}\delta\beta \tag{22}$$

where

$$\frac{\partial F(X;\alpha_0,\beta_0)}{\partial\alpha} = \int_0^X \frac{\partial f(x;\alpha,\beta)}{\partial\alpha}\Big|_{\alpha=\alpha_0} dx \tag{23}$$

and

$$\frac{\partial F(X;\alpha_0,\beta_0)}{\partial\beta} = \int_0^X \frac{\partial f(x;\alpha,\beta)}{\partial\beta}\Big|_{\beta=\beta_0} dx. \tag{24}$$

Equation (22) is linear in $\delta\alpha$ and $\delta\beta$.

Let Q represent the sum of the squares of the differences between the analytical, $F(X_i;\ \alpha,\ \beta)$, and observed cumulative, P_i, distributions given by

$$Q = \sum_1^N [F(X_i;\alpha,\beta) - P_i]^2. \tag{25}$$

Replacing $F(X_i;\ \alpha,\ \beta)$ by the expression in equation (22) gives

$$Q = \sum_1^N [F(X_i;\alpha_0,\beta_0) + \frac{\partial F(X_i;\alpha_0,\beta_0)}{\partial\alpha}\delta\alpha + \frac{\partial F(X_i;\alpha_0,\beta_0)}{\partial\beta}\delta\beta - P_i]^2 \ . \tag{26}$$

Taking the partial derivatives of Q with respect to $\delta\alpha$ and $\delta\beta$ and setting each derivative equal to zero to find a minimum of Q give

$$\sum_1^N [\frac{\partial F_0(X_i)}{\partial\alpha}]^2\delta\alpha + \sum_1^N [\frac{\partial F_0(X_i)}{\partial\alpha}\frac{\partial F_0(X_i)}{\partial\beta}]\delta\beta = \sum_1^N [P_i - F_0(X_i)]\frac{\partial F_0(X_i)}{\partial\alpha} \tag{27}$$

and

$$\sum_{1}^{N} \left[\frac{\partial F_0(X_i)}{\partial \alpha} \frac{\partial F_0(X_i)}{\partial \beta} \right] \delta\alpha + \sum_{1}^{N} \left[\frac{\partial F_0(X_i)}{\partial \beta} \right]^2 \delta\beta = \sum_{1}^{N} \left[P_i - F_0(X_i) \right] \frac{\partial F_0(X_i)}{\partial \beta} \tag{28}$$

where the terms involving $F_0(X_i)$ and its partial derivatives denote the function $F(x;\ \alpha,\ \beta)$ and its partial derivatives evaluated at X_i, α_0, and β_0. These two equations are linear in $\delta\alpha$ and $\delta\beta$.

The nonlinear least squares fit procedure begins by getting initial values for α_0 and β_0; solving equations (27) and (28) for $\delta\alpha$ and $\delta\beta$ using the definitions in equations (18), (23), and (24); and getting updated values of α and β according to the iterative equations

$$\alpha_k = \alpha_{k-1} + \delta\alpha \tag{29}$$

and

$$\beta_k = \beta_{k-1} + \delta\beta \tag{30}$$

for k = 1, 2, ... until $\delta\alpha$ and $\delta\beta$ become very small and convergence is obtained. The initial values of the parameters may be selected by any method. Reasonable initial values are obtained by using the method of moments to get α_0 and β_0.

5. WIND SPEED DISTRIBUTIONS

All three of the analytical distributions considered in this analysis have zero probability of occurrence at x = 0. The observed wind speed, however, may be calm or zero. To account for this phenomenon in all weather classes except WXCL-4 and WXCL-5 (advective fog cases), the wind speed cumulative distribution is defined by the equation

$$W(X; p_0, \alpha, \beta) = p_0 \delta(0) + (1 - p_0) F(X; \alpha, \beta) \tag{31}$$

where X is the wind speed, $\delta(0)$ is the Dirac delta function, p_0 is the probability of calm wind speeds, and $F(X;\ \alpha,\ \beta)$ is the appropriate analytical cumulative distribution function.

For weather classes WXCL-4 and WXCL-5, the wind speed cumulative distribution is defined by a modification of the previous equation to give

$$W(X; p_0, \alpha, \beta) = (1 - p_0) F(X - 3; \alpha, \beta) \tag{32}$$

where the wind speed, X, is at least 3.5 m/s. The probabilities of calm wind speeds for each region, time period, and weather class combination are listed in table 5. Similarly, the numbers of noncalm wind speed observations are listed in table 6.

TABLE 5. PROBABILITIES OF CALM WIND SPEEDS FOR ALL WIND SPEED DISTRIBUTION CASES

Region	Season	Time Period	Wx Class	Probability (%)
European Lowlands	Winter	All Hours	WXCL-1	5.33310
			WXCL-2	3.33883
			WXCL-3	1.82471
			WXCL-4	0.00000
			WXCL-6	19.41515
			WXCL-7	15.16001
European Lowlands	Annual	All Hours	WXCL-1	6.81479
			WXCL-2	3.60214
			WXCL-3	1.90912
			WXCL-4	0.00000
			WXCL-6	20.65096
			WXCL-7	17.10452
European Highlands	Winter	All Hours	WXCL-1	16.06559
			WXCL-2	8.78897
			WXCL-3	4.84744
			WXCL-4	0.00000
			WXCL-5	0.00000
			WXCL-6	29.69938
			WXCL-7	22.04064
European Highlands	Annual	All Hours	WXCL-1	17.58078
			WXCL-2	8.42896
			WXCL-3	4.43246
			WXCL-4	0.00000
			WXCL-5	0.00000
			WXCL-6	35.54087
			WXCL-7	25.42562
Mideast Desert	Summer	Night	WXCL-1	14.88957
			WXCL-8	8.10640
			WXCL-9	15.84338
Mideast Desert	Summer	Day	WXCL-1	13.15426
			WXCL-8	6.31811
			WXCL-9	12.18719
Mideast Desert	Annual	Night	WXCL-1	21.29619
			WXCL-8	7.62053
			WXCL-9	21.73497
Mideast Desert	Annual	Day	WXCL-1	17.75504
			WXCL-8	6.83641
			WXCL-9	16.04527

TABLE 6. THE NUMBER OF NONCALM WIND SPEED OBSERVATIONS FOR ALL WIND SPEED DISTRIBUTION CASES

Region	Season	Time Period	Wx Class	Noncalm Count
European Lowlands	Winter	All Hours	WXCL-1	54211
			WXCL-2	230939
			WXCL-3	73280
			WXCL-4	3621
			WXCL-6	10775
			WXCL-7	14528
European Lowlands	Annual	All Hours	WXCL-1	222626
			WXCL-2	642539
			WXCL-3	171815
			WXCL-4	5456
			WXCL-6	21990
			WXCL-7	27736
European Highlands	Winter	All Hours	WXCL-1	31838
			WXCL-2	182433
			WXCL-3	62402
			WXCL-4	4753
			WXCL-5	217
			WXCL-6	9705
			WXCL-7	14502
European Highlands	Annual	All Hours	WXCL-1	137153
			WXCL-2	504420
			WXCL-3	141439
			WXCL-4	9842
			WXCL-5	277
			WXCL-6	16089
			WXCL-7	26019
Mideast Desert	Summer	Night	WXCL-1	44780
			WXCL-8	1451
			WXCL-9	18979
Mideast Desert	Summer	Day	WXCL-1	84355
			WXCL-8	8081
			WXCL-9	39687
Mideast Desert	Annual	Night	WXCL-1	138562
			WXCL-8	6534
			WXCL-9	84275
Mideast Desert	Annual	Day	WXCL-1	193413
			WXCL-8	24516
			WXCL-9	133441

The observed probability distribution was obtained by forming histograms of frequency of occurrence of observed wind speed with all histogram interval widths being 0.5 m/s. The histogram frequencies of occurrence were converted to probabilities and assigned to the wind speeds at the midpoints of the intervals. The corresponding analytical probability distribution was obtained by evaluating the analytical cumulative probability distribution at the wind speeds corresponding to the beginning and end of each histogram interval and using the difference between the two values assigned to the wind speed at the midpoint of the interval.

The mean absolute deviation between the observed and analytical cumulative distributions for each region, time period, and weather class combination is listed in table 7. Similarly, the rms deviation between the cumulative distributions is listed in table 8. Generally, both the mean absolute deviations and the rms deviations are small, indicating the analytical distributions adequately represent the observed wind speed distributions. The names of the corresponding best distribution are listed in table 9.

6. ANALYSIS RESULTS

6.1 European Lowlands

The observed noncalm wind speed and analytical distributions along with the observed and analytical cumulative distributions for the European Lowlands are depicted in figures 1 through 12. The figures correspond to winter and annual time periods for weather classes WXCL-1 to WXCL-4, WXCL-6, and WXCL-7. Weather class WXCL-5 had an insufficient number of observations for analysis. The odd numbered figures depict the observed and analytical distributions, and the even number figures depict the observed and analytical cumulative distributions. In each figure the differences between the observed and analytical values are also plotted. The observed distributions are plotted using a dashed line, analytical distributions with a solid line, and the difference between them with a dotted line.

The figures depict only the noncalm part of the wind speed distributions. The number of noncalm wind observations used to fit the analytical distributions to the observed wind speed distributions is displayed in each figure. In addition, the best analytical probability distribution and the corresponding scale and shape parameters are listed in each figure.

Of the 12 different weather class and season combinations there were 3 cases where the gamma distribution was the best, 3 for the log-normal and 6 for the Weibull (reference table 9). The log-normal distribution was the best for weather class WXCL-4 (advective fog case) and the annual wind speed distribution for WXCL-7 (fog). The gamma distribution was the best for the winter wind speed distributions for WXCL-1, WXCL-2, and WXCL-7. Overall, the analytical distributions perform well at describing the observed wind speed distributions. The worst performance was for the weather classes involving fog. Even for those cases the analytical distributions perform fairly well.

6.2 European Highlands

Figures 13 through 26 depict the same type of wind speed information for the European Highlands. For this region weather class WXCL-5 had enough noncalm wind speed observations to be analyzed. Of the 14 different weather class and season combinations there were 2 cases where the gamma distribution was the best, 10 for the log-normal and 2 for the Weibull (reference table 9). The gamma distribution was best for the winter wind speed distributions for WXCL-5 (advective fog and precipitation) and WXCL-6 (radiative fog). The Weibull distribution was the best for weather class WXCL-4 (advective fog). Overall, the analytical distributions performed fairly well for all cases except WXCL-4 and WXCL-7. Again, the analytical distributions for weather classes involving fog proved to have the worst performance, with WXCL-4 and WXCL-7 being unsuited for analytical distribution representation.

6.3 Mideast Desert

Figures 27 through 38 depict the same type of wind speed information for the Mideast Desert region, except that the distributions are for weather classes WXCL-1, WXCL-8, and WXCL-9 and the time periods are summer and annual for night and daytime. Of the 12 different weather class and time period combinations there were 2 cases where the gamma distribution was the best and 10 for the Weibull (reference table 9). The gamma distribution was the best during the annual night period for WXCL-1 (no clouds) and WXCL-9 (low visibility). For the Mideast the observed wind speed distributions are more "lumpy" than those for the European regions. However, the analytical distributions appear to adequately represent the observed distributions. The worst representations occur for the daytime dust storm conditions (WXCL-8) when the wind speeds tend to be greater and more variable.

7. CONCLUSIONS

The observed wind speed distributions are adequately represented by the analytical distributions except in a few cases. For these exceptions, weather classes WXCL-4 and WXCL-7 for the European Highlands, the observed wind speed distributions do not lend themselves to analytical representation with enough accuracy to be useful. The PM-BAT intends to use the analytical distributions to generate wind speeds by pseudorandom numbers. For the two exception cases, the observed wind speed empirical distributions should be used rather than the analytical distributions to generate random wind speeds. In all cases whether analyti' .1 or empirical distributions are used, generated wind speeds more than 40 m/s should be discarded. Furthermore, occurrences of such large values of wind speed may indicate a problem with the pseudorandom number generator.

TABLE 7. THE MEAN ABSOLUTE DEVIATION BETWEEN THE OBSERVED AND ANALYTICAL CUMULATIVE DISTRIBUTIONS

Region	Season	Time Period	Wx Class	Mean Abs Dev (%)
European Lowlands	Winter	All Hours	WXCL-1	0.29212
			WXCL-2	0.29047
			WXCL-3	0.30860
			WXCL-4	0.38378
			WXCL-6	3.47584
			WXCL-7	0.43066
European Lowlands	Annual	All Hours	WXCL-1	0.36995
			WXCL-2	0.39851
			WXCL-3	0.32126
			WXCL-4	0.31072
			WXCL-6	3.28172
			WXCL-7	0.32688
European Highlands	Winter	All Hours	WXCL-1	0.33095
			WXCL-2	0.55635
			WXCL-3	0.77190
			WXCL-4	3.59613
			WXCL-5	1.78300
			WXCL-6	3.00902
			WXCL-7	2.29373
European Highlands	Annual	All Hours	WXCL-1	0.29323
			WXCL-2	0.49851
			WXCL-3	0.65162
			WXCL-4	2.82679
			WXCL-5	1.80694
			WXCL-6	2.81105
			WXCL-7	2.29231
Mideast Desert	Summer	Night	WXCL-1	0.46519
			WXCL-8	0.58164
			WXCL-9	0.46327
Mideast Desert	Summer	Day	WXCL-1	0.44986
			WXCL-8	0.97730
			WXCL-9	0.38925
Mideast Desert	Annual	Night	WXCL-1	0.38754
			WXCL-8	0.47509
			WXCL-9	0.36817
Mideast Desert	Annual	Day	WXCL-1	0.47917
			WXCL-8	0.73087
			WXCL-9	0.40136

TABLE 8. THE ROOT-MEAN-SQUARE DEVIATION BETWEEN THE OBSERVED AND ANALYTICAL CUMULATIVE DISTRIBUTIONS

Region	Season	Time Period	Wx Class	RMS Dev (%)
European Lowlands	Winter	All Hours	WXCL-1	0.58660
			WXCL-2	0.54364
			WXCL-3	0.51059
			WXCL-4	0.95719
			WXCL-6	3.81003
			WXCL-7	0.96541
European Lowlands	Annual	All Hours	WXCL-1	0.76201
			WXCL-2	0.78650
			WXCL-3	0.57538
			WXCL-4	0.86317
			WXCL-6	3.55605
			WXCL-7	0.80706
European Highlands	Winter	All Hours	WXCL-1	0.59869
			WXCL-2	0.78476
			WXCL-3	1.05942
			WXCL-4	4.25872
			WXCL-5	2.37126
			WXCL-6	3.48083
			WXCL-7	3.15858
European Highlands	Annual	All Hours	WXCL-1	0.64867
			WXCL-2	0.73165
			WXCL-3	0.89949
			WXCL-4	3.24614
			WXCL-5	2.02381
			WXCL-6	3.48151
			WXCL-7	2.92015
Mideast Desert	Summer	Night	WXCL-1	0.88549
			WXCL-8	0.95012
			WXCL-9	0.74849
Mideast Desert	Summer	Day	WXCL-1	0.85728
			WXCL-8	1.78054
			WXCL-9	0.67480
Mideast Desert	Annual	Night	WXCL-1	0.81240
			WXCL-8	0.66669
			WXCL-9	0.72328
Mideast Desert	Annual	Day	WXCL-1	0.91409
			WXCL-8	1.22850
			WXCL-9	0.71903

TABLE 9. THE NAMES OF THE BEST ANALYTICAL DISTRIBUTIONS TO REPRESENT THE OBSERVED WIND SPEED DISTRIBUTIONS

Region	Season	Time Period	Wx Class	Distribution
European Lowlands	Winter	All Hours	WXCL-1	Gamma
			WXCL-2	Gamma
			WXCL-3	Weibull
			WXCL-4	Log-Normal
			WXCL-6	Weibull
			WXCL-7	Gamma
European Lowlands	Annual	All Hours	WXCL-1	Weibull
			WXCL-2	Weibull
			WXCL-3	Weibull
			WXCL-4	Log-Normal
			WXCL-6	Weibull
			WXCL-7	Log-Normal
European Highlands	Winter	All Hours	WXCL-1	Log-Normal
			WXCL-2	Log-Normal
			WXCL-3	Log-Normal
			WXCL-4	Weibull
			WXCL-5	Gamma
			WXCL-6	Gamma
			WXCL-7	Log-Normal
European Highlands	Annual	All Hours	WXCL-1	Log-Normal
			WXCL-2	Log-Normal
			WXCL-3	Log-Normal
			WXCL-4	Weibull
			WXCL-5	Log-Normal
			WXCL-6	Log-Normal
			WXCL-7	Log-Normal
Mideast Desert	Summer	Night	WXCL-1	Weibull
			WXCL-8	Weibull
			WXCL-9	Weibull
Mideast Desert	Summer	Day	WXCL-1	Weibull
			WXCL-8	Weibull
			WXCL-9	Weibull
Mideast Desert	Annual	Night	WXCL-1	Gamma
			WXCL-8	Weibull
			WXCL-9	Gamma
Mideast Desert	Annual	Day	WXCL-1	Weibull
			WXCL-8	Weibull
			WXCL-9	Weibull

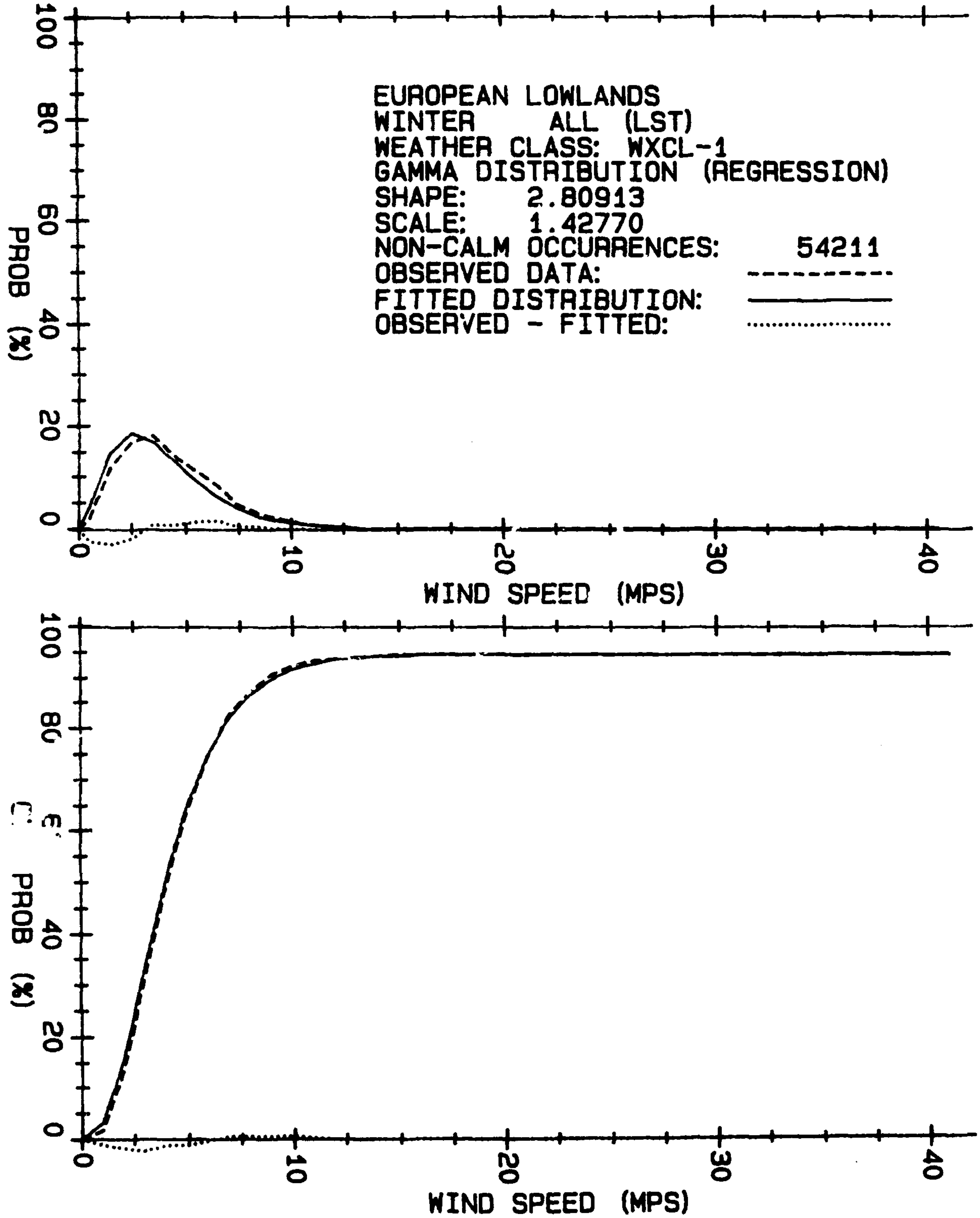

Figure 1. Regression fitted gamma distribution for European Lowlands winter wind speeds for we ther class 1.

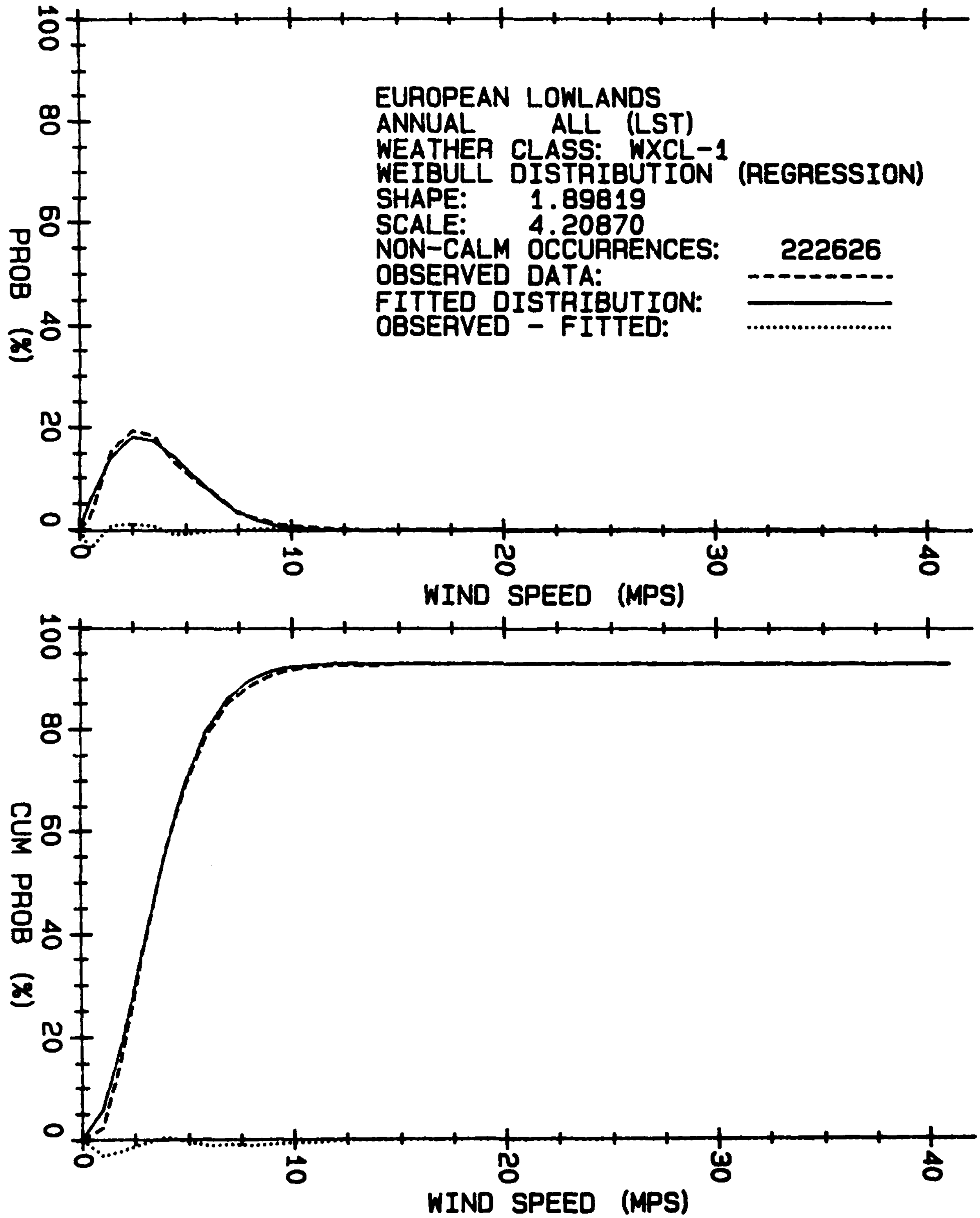

Figure 2. Regression fitted Weibull distribution for European Lowlands wind speeds for weather class 1.

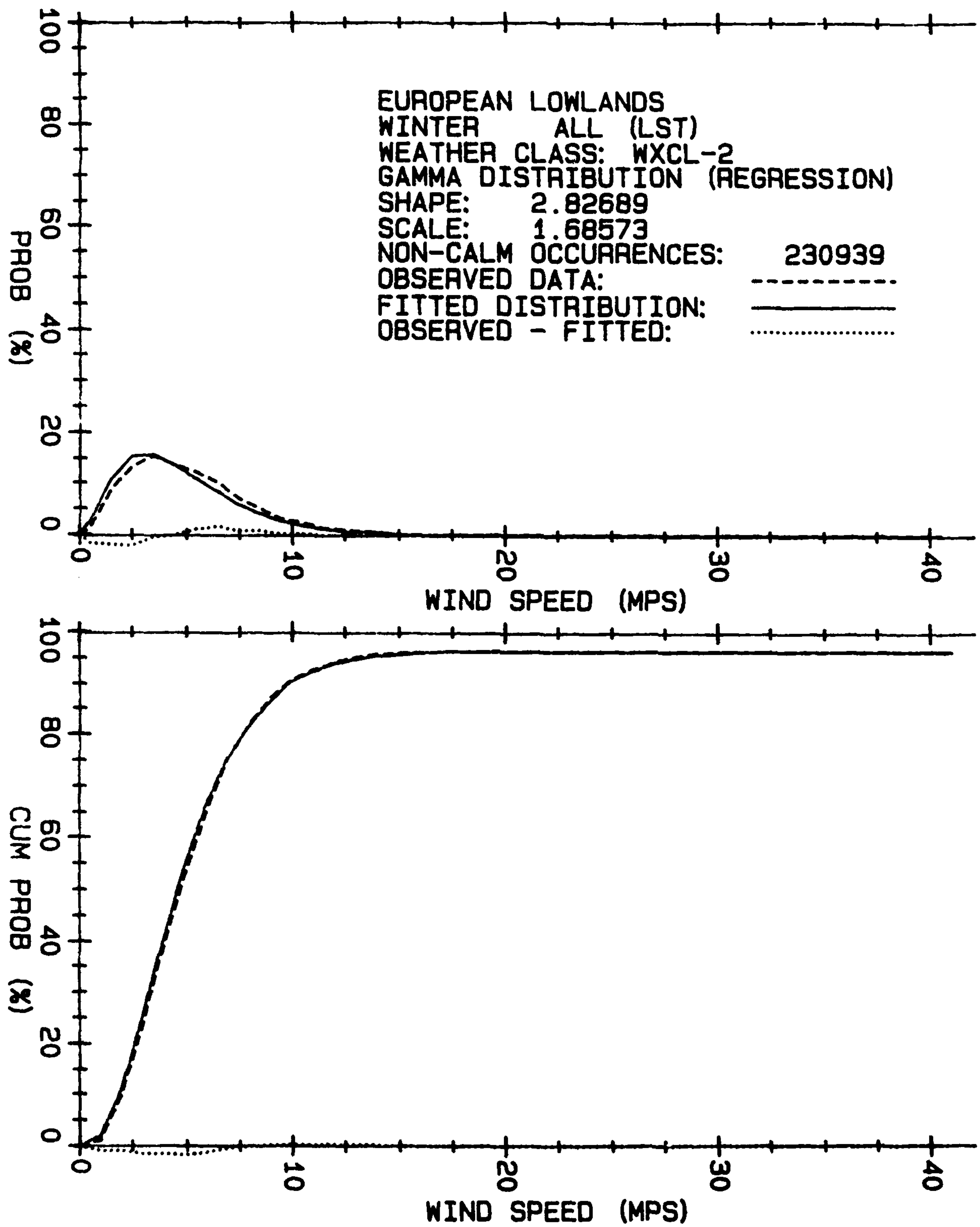

Figure 3. Regression fitted gamma distribution for European Lowlands winter wind speeds for weather class 2.

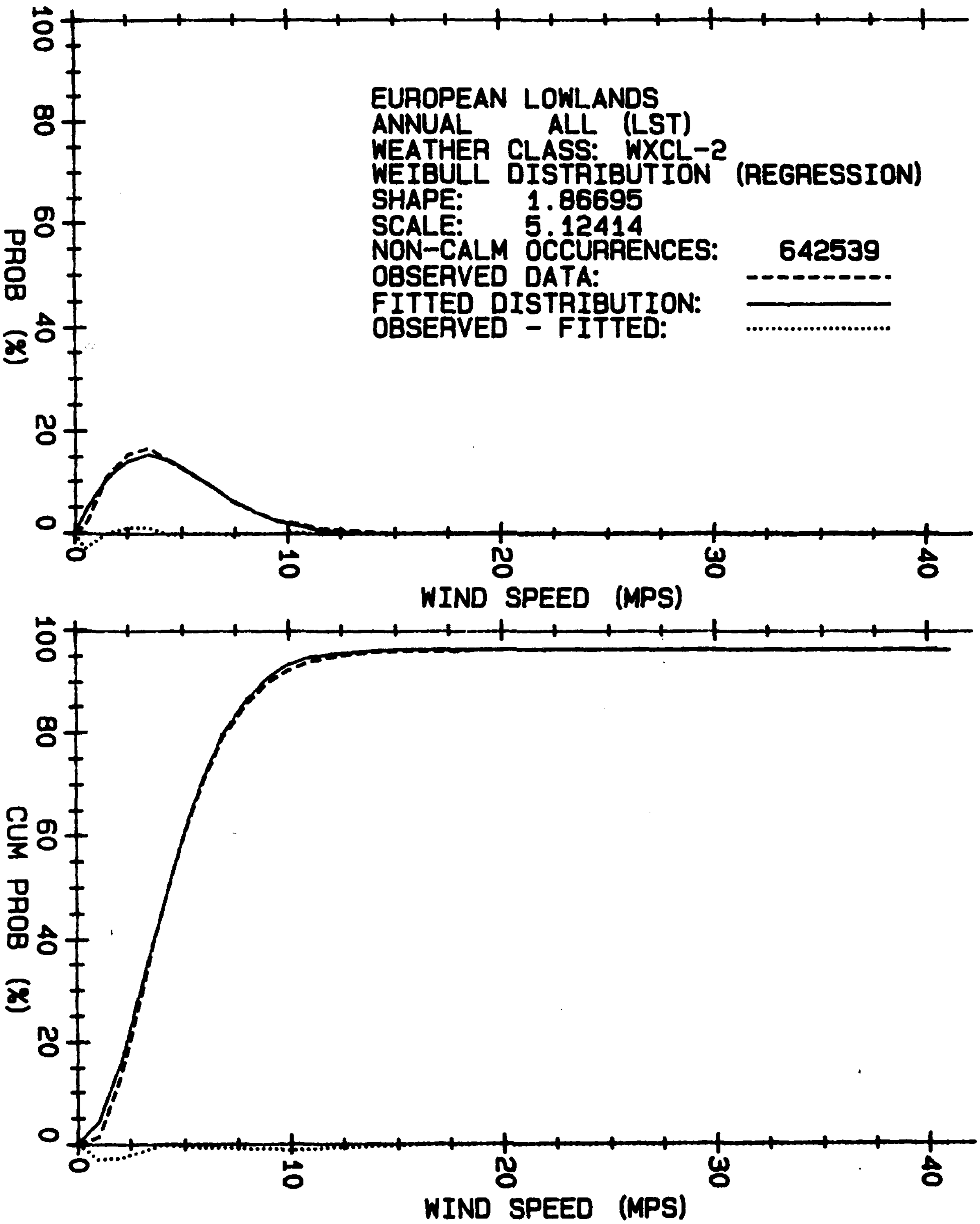

Figure 4. Regression fitted Weibull distribution for European Lowlands wind speeds for weather class 2.

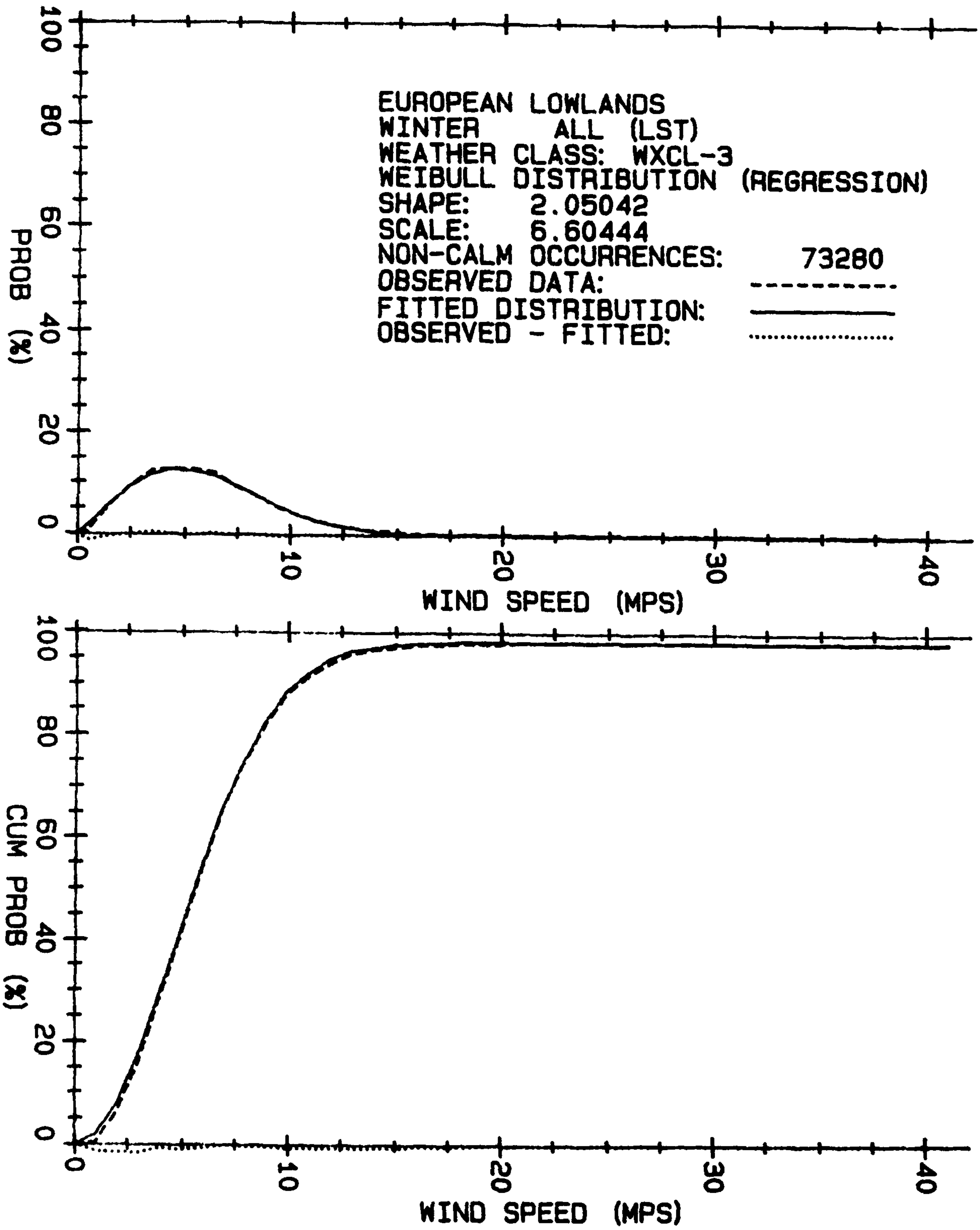

Figure 5. Regression fitted Weibull distribution for European Lowlands winter wind speeds for weather class 3.

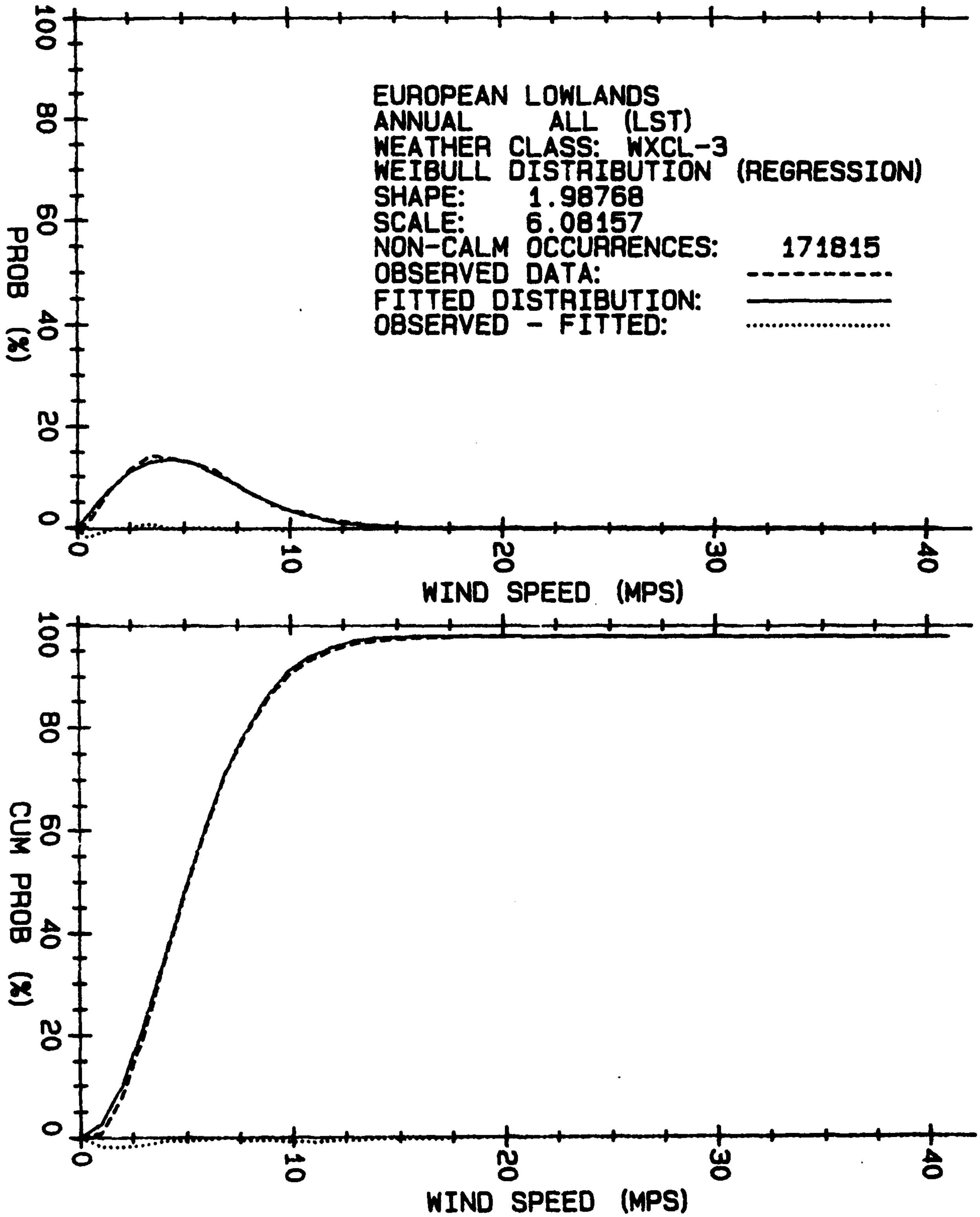

Figure 6. Regression fitted Weibull distribution for European Lowlands wind speeds for weather class 3.

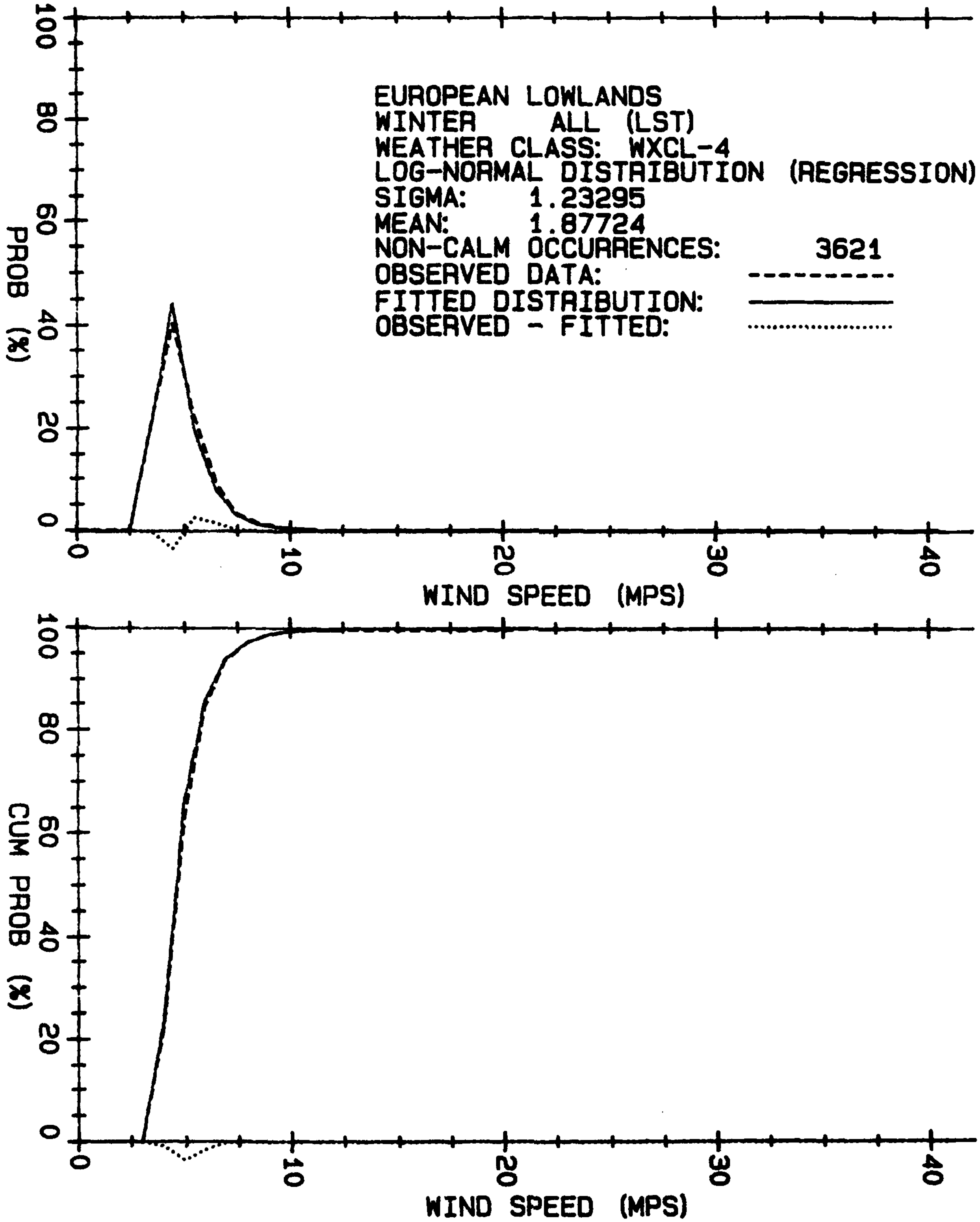

Figure 7. Regression fitted log-normal distribution for European Lowlands winter wind speeds for weather class 4.

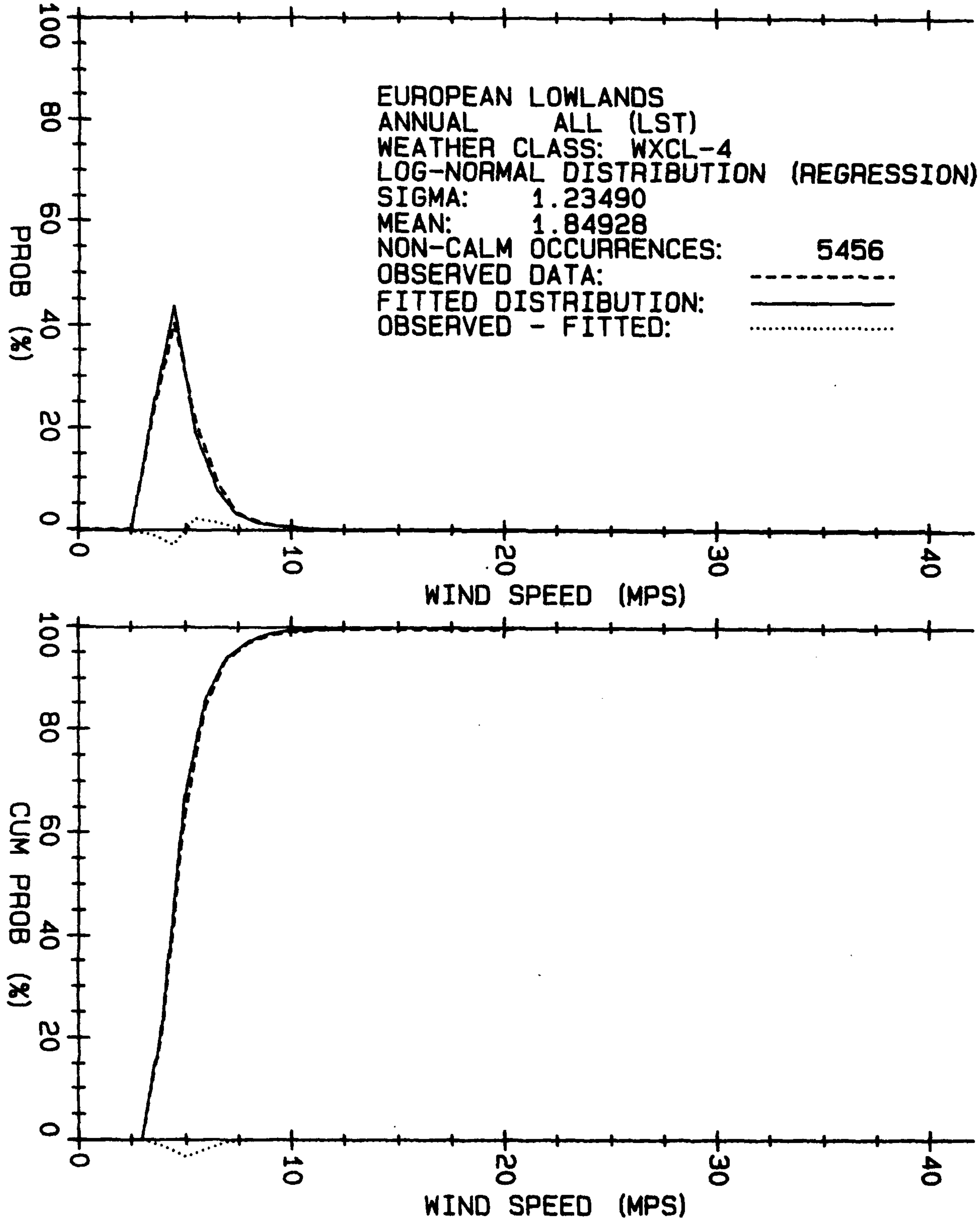

Figure 8. Regression fitted log-normal distribution for European Lowlands wind speeds for weather class 4.

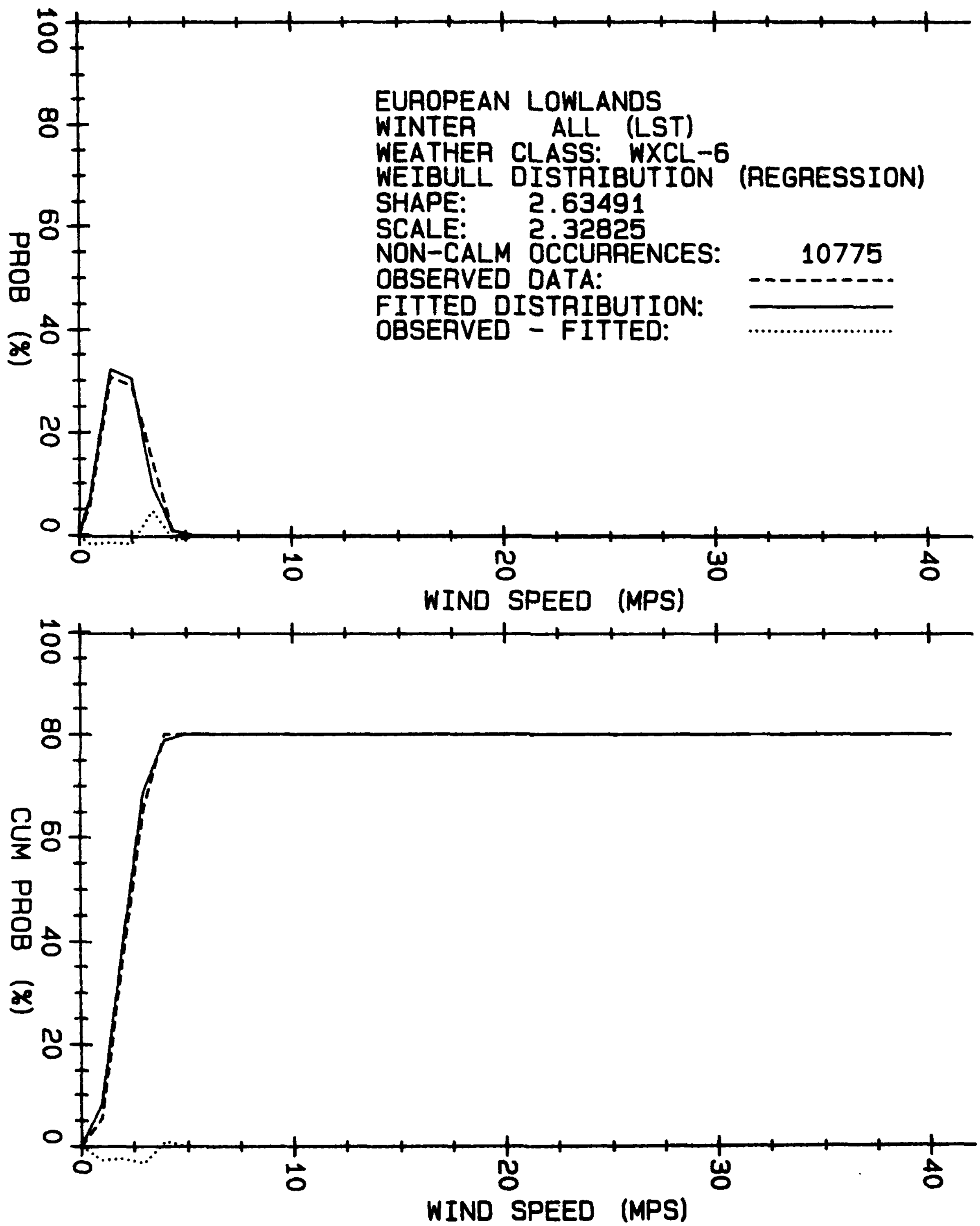

Figure 9. Regression fitted Weibull distribution for European Lowlands winter wind speeds for weather class 6.

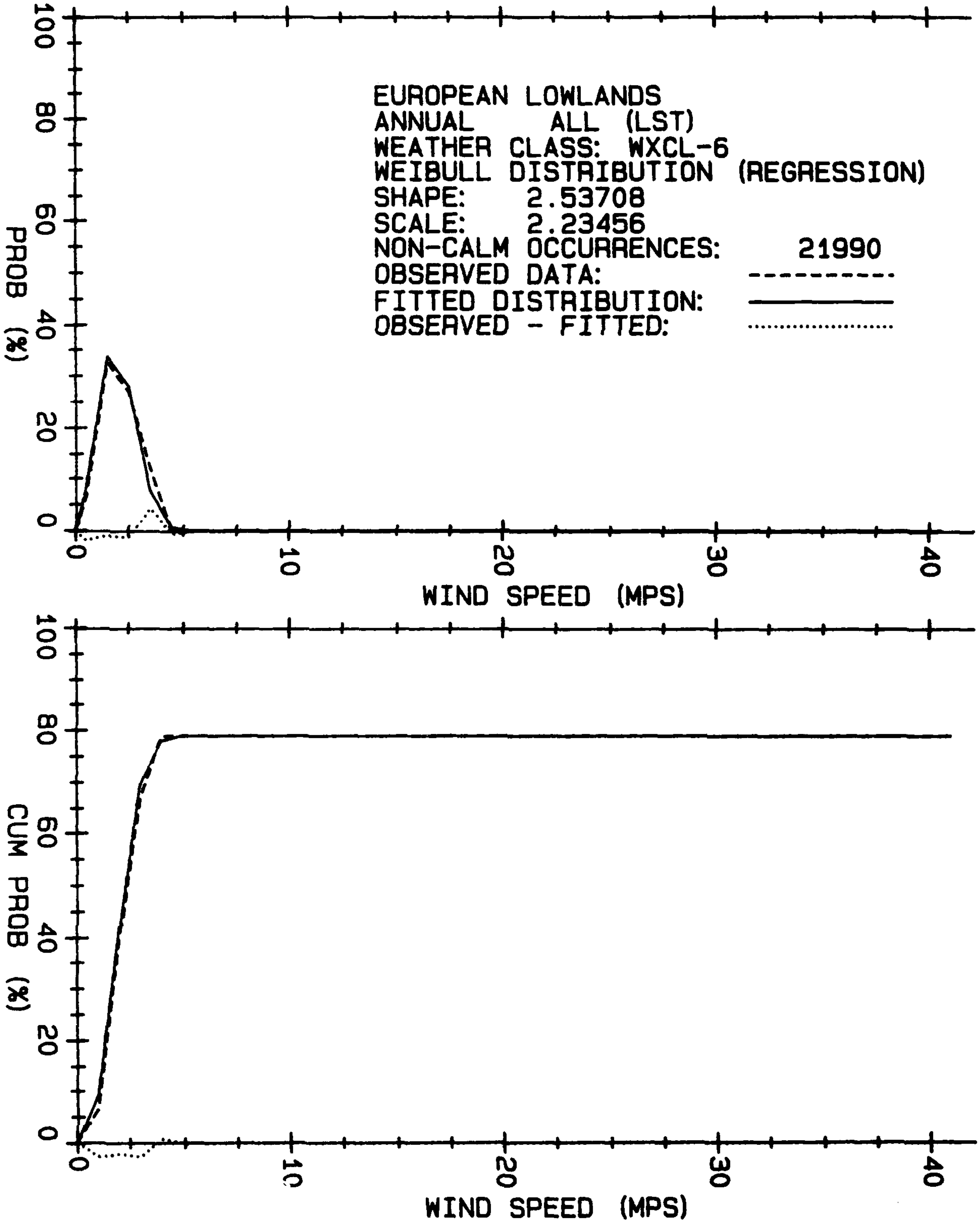

Figure 10. Regression fitted Weibull distribution for European Lowlands wind speeds for weather class 6.

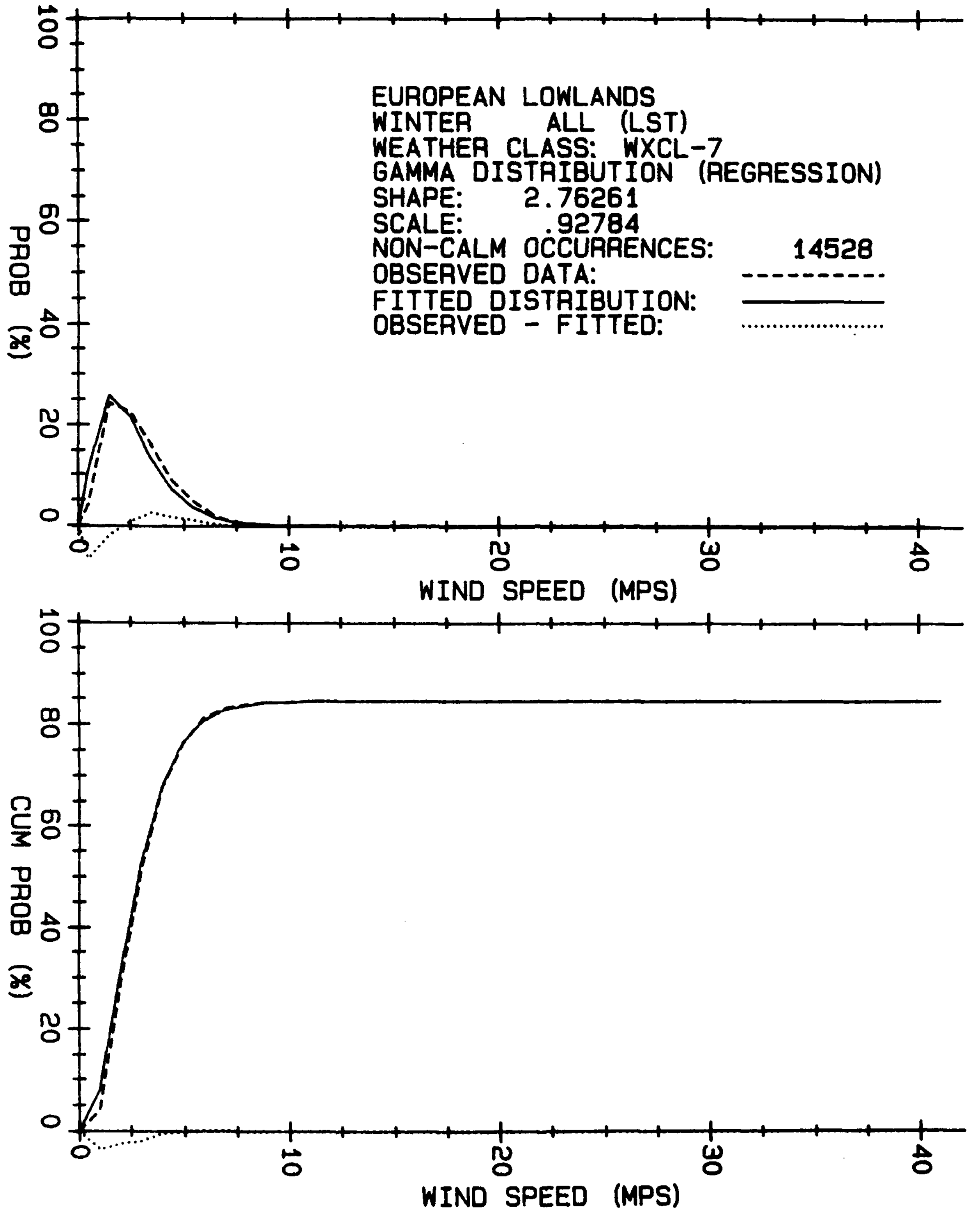

Figure 11. Regression fitted gamma distribution for European Lowlands winter wind speeds for weather class 7.

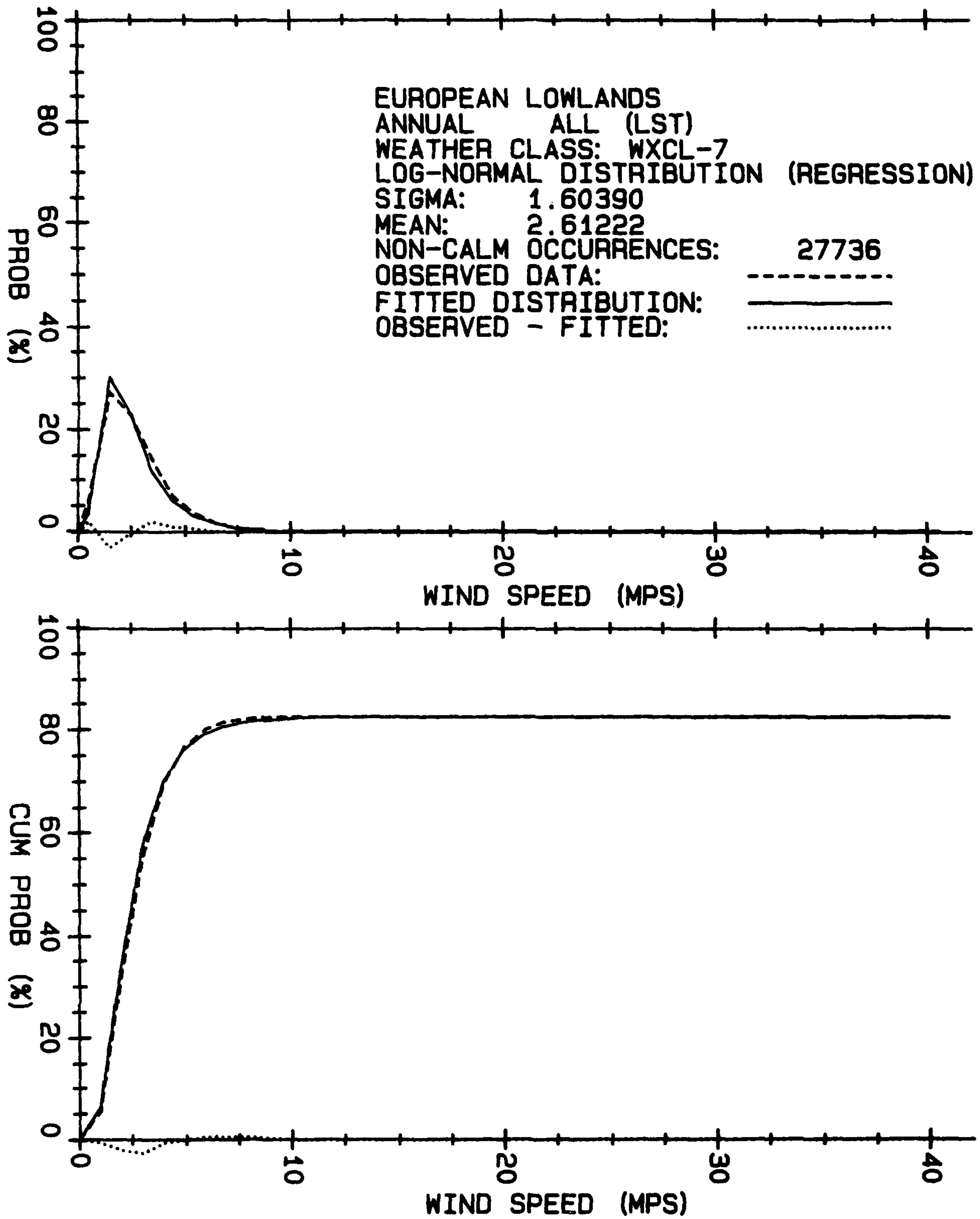

Figure 12. Regression fitted log-normal distribution for European Lowlands wind speeds for weather class 7.

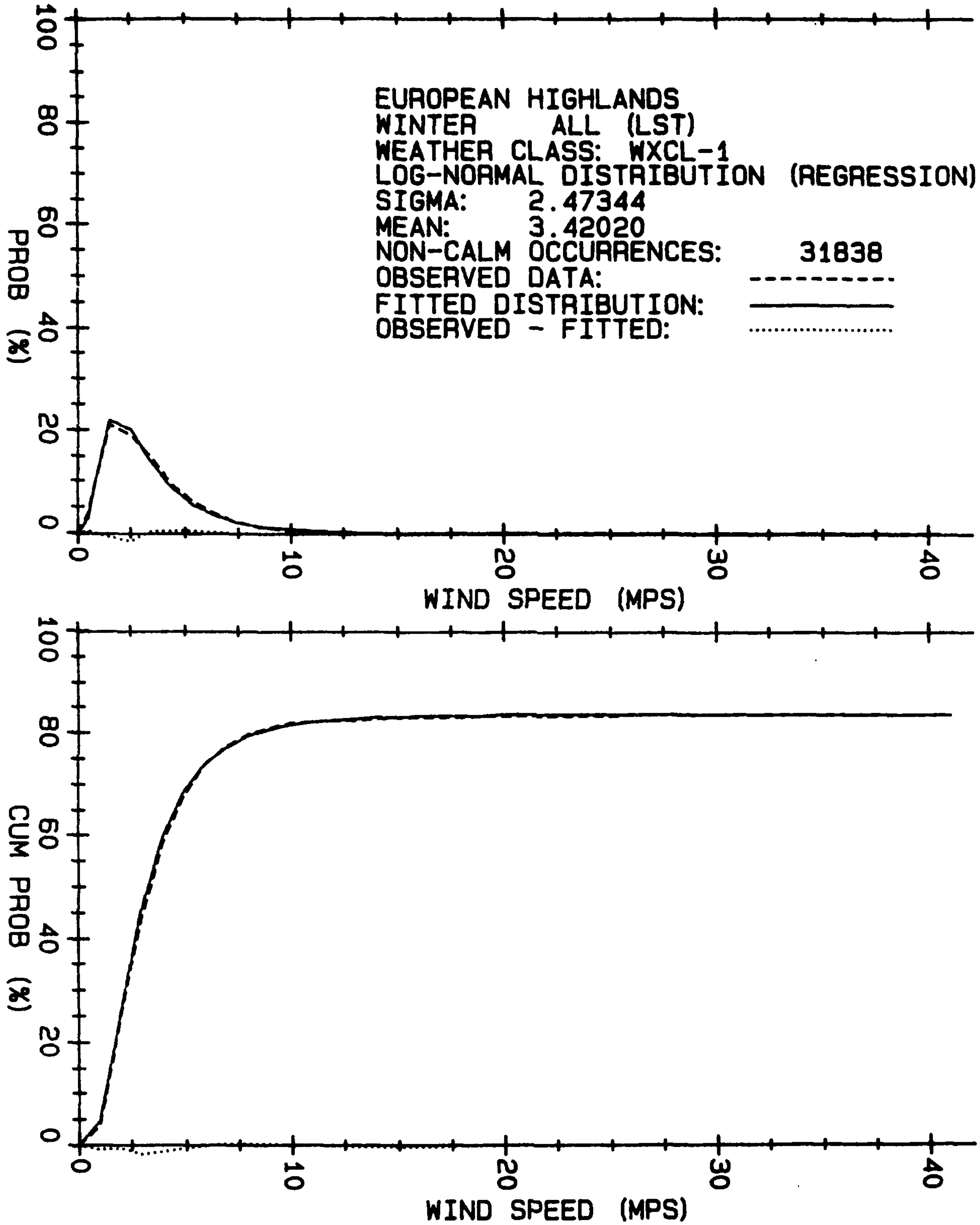

Figure 13. Regression fitted log-normal distribution for European Highlands winter wind speeds for weather class 1.

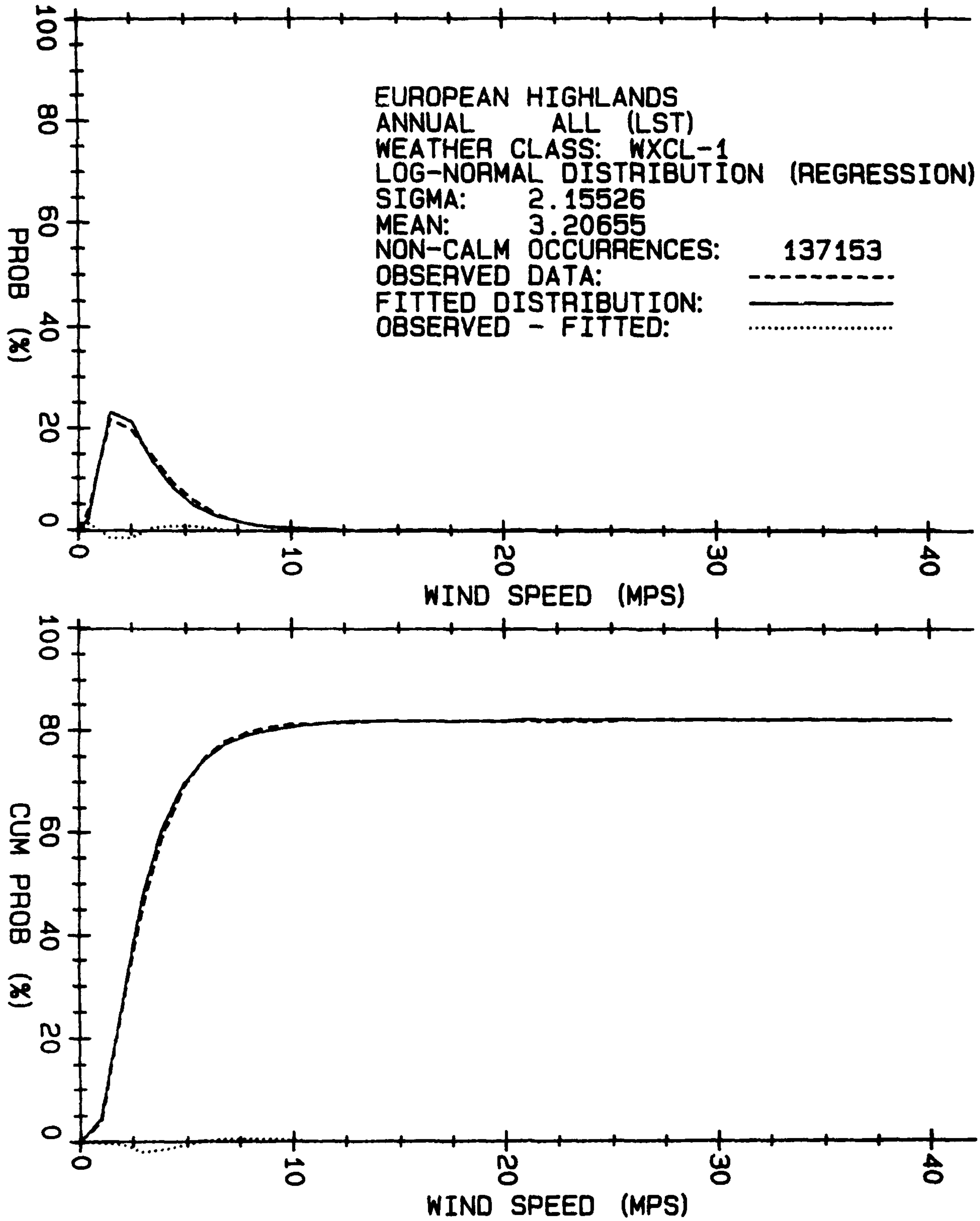

Figure 14. Regression fitted log-normal distribution for European Highlands wind speeds for weather class 1.

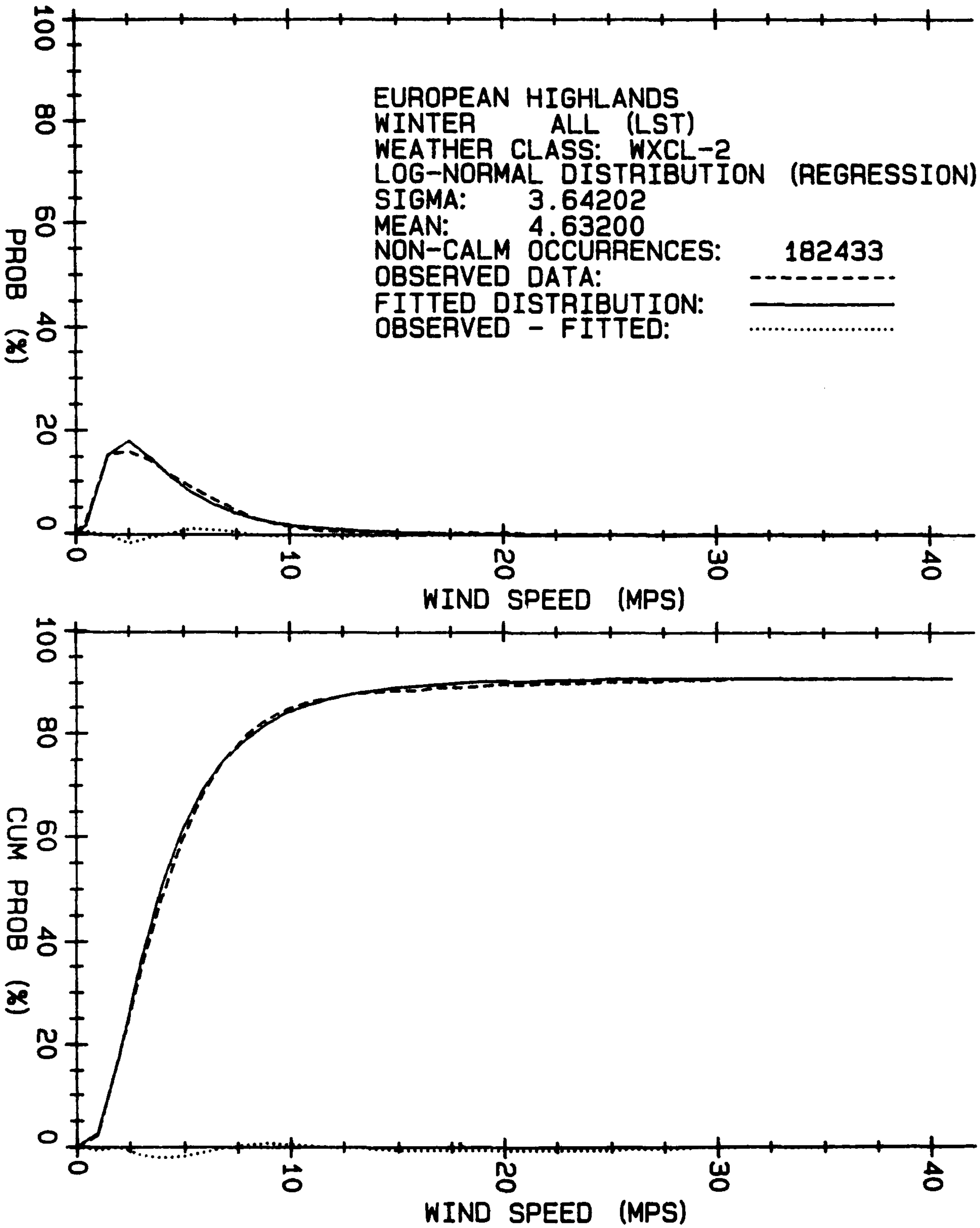

Figure 15. Regression fitted log-normal distribution for European Highlands winter wind speeds for weather class 2.

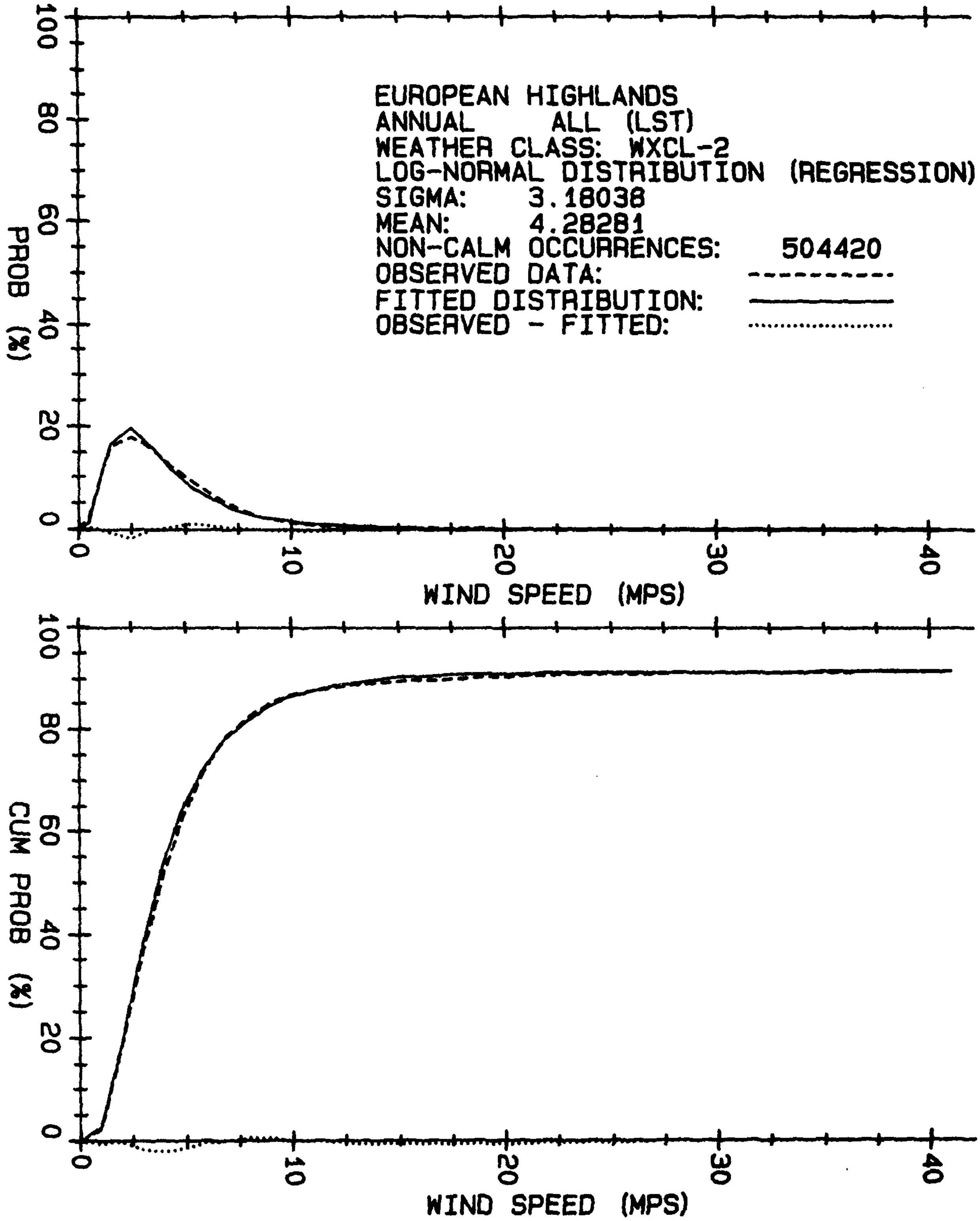

Figure 16. Regression fitted log-normal distribution for European Highlands wind speeds for weather class 2.

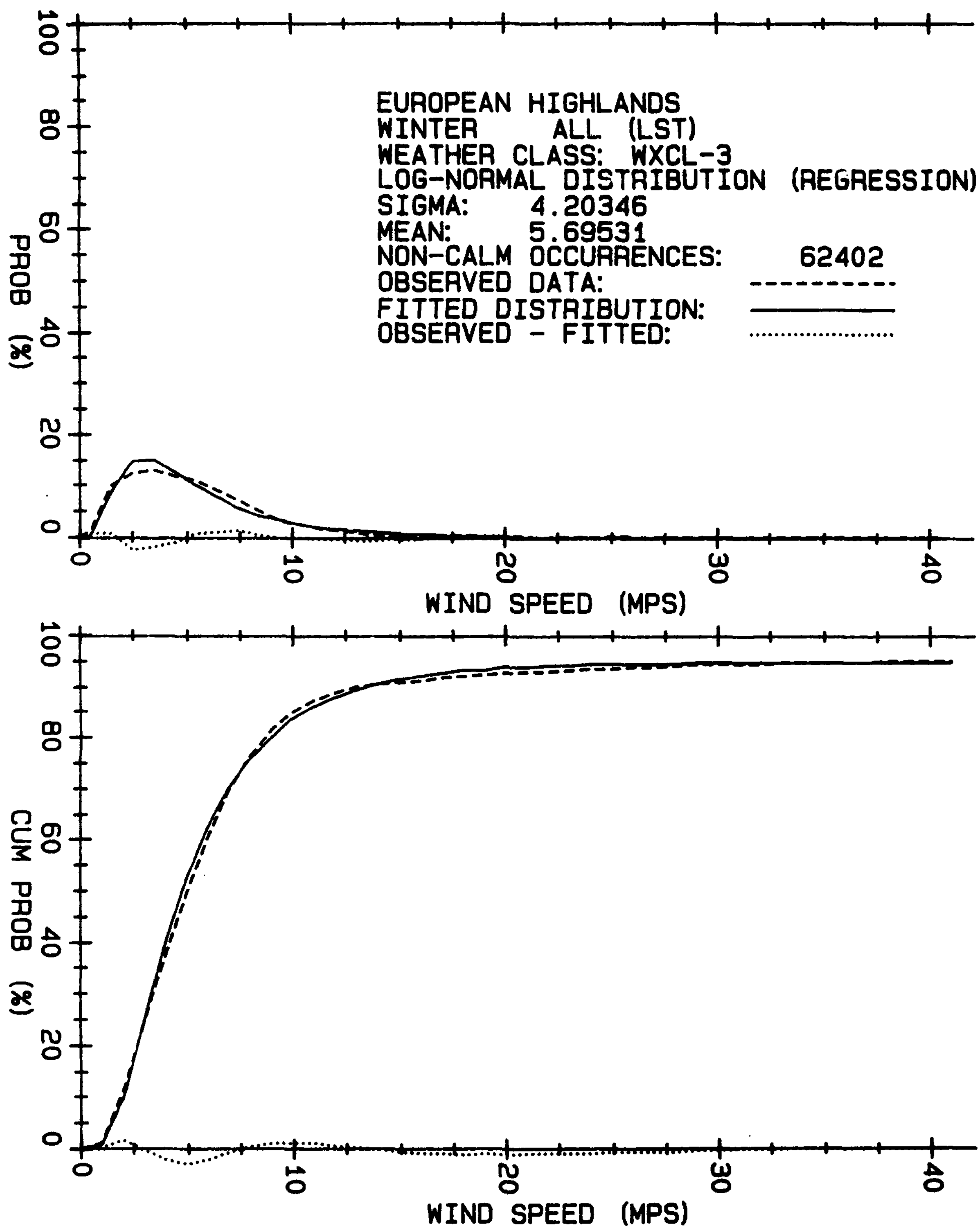

Figure 17. Regression fitted log-normal distribution for European Highlands winter wind speeds for weather class 3.

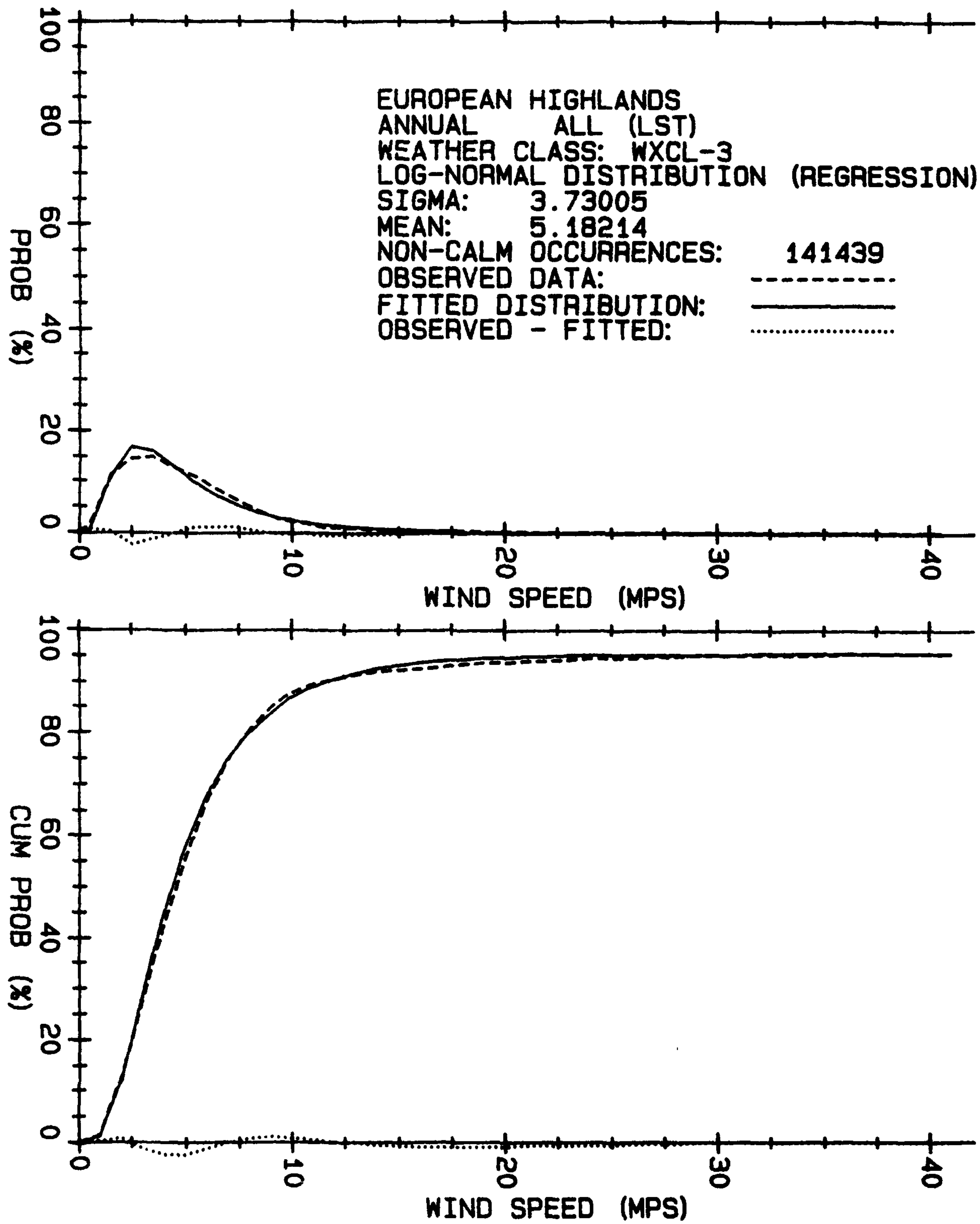

Figure 18. Regression fitted log-normal distribution for European Highlands wind speeds for weather class 3.

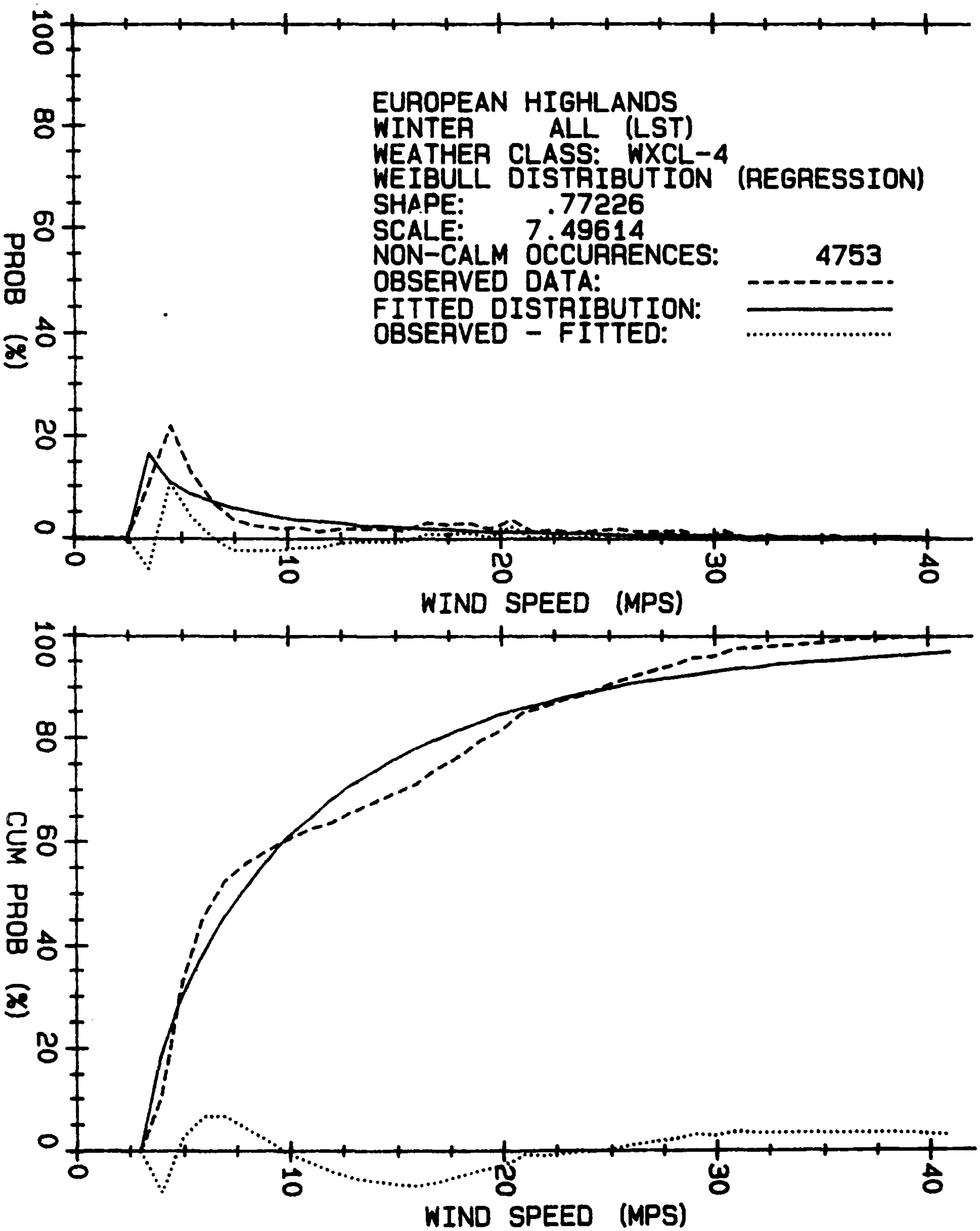

Figure 19. Regression fitted Weibull distribution for European Highlands winter wind speeds for weather class 4.

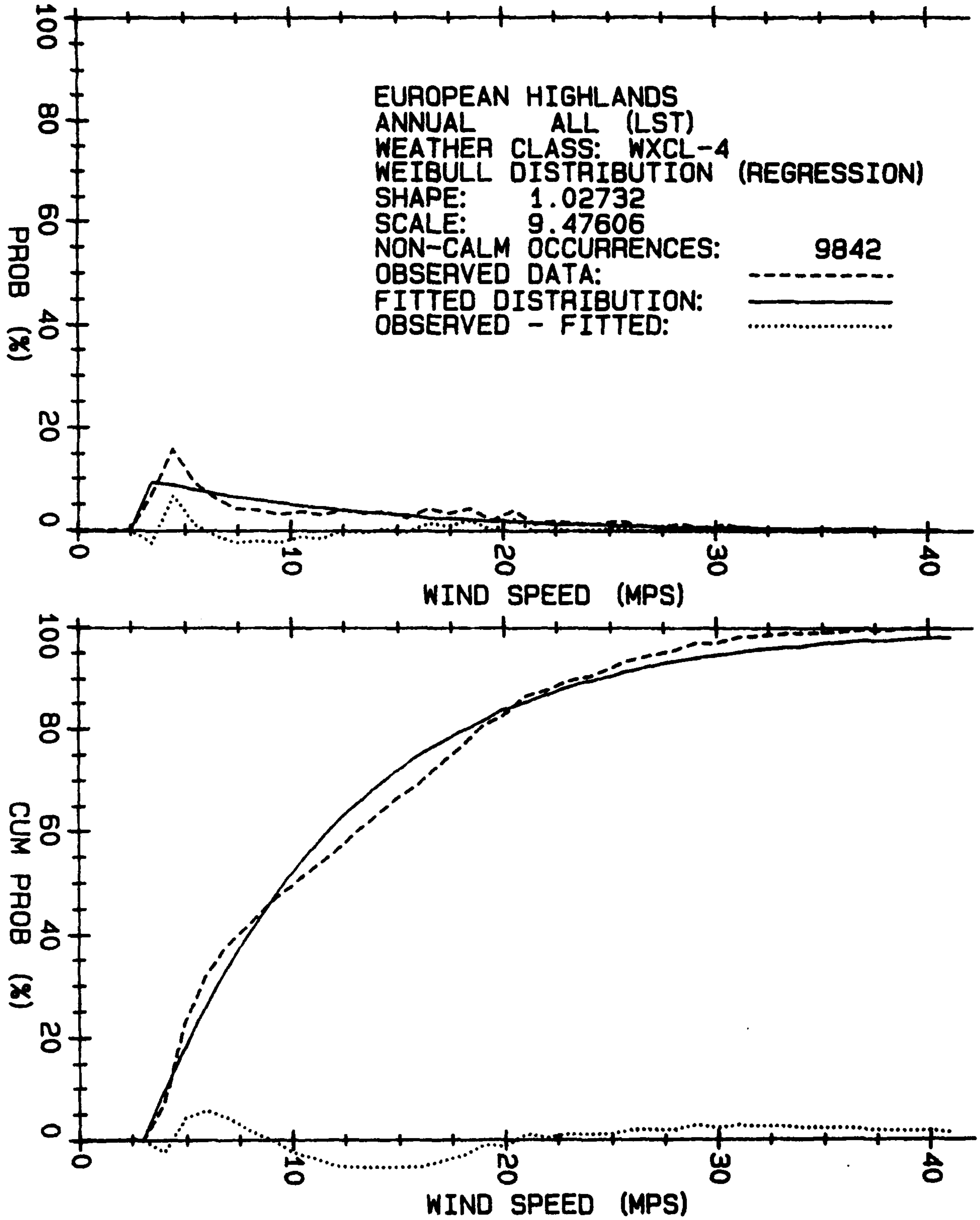

Figure 20. Regression fitted Weibull distribution for European Highlands wind speeds for weather class 4.

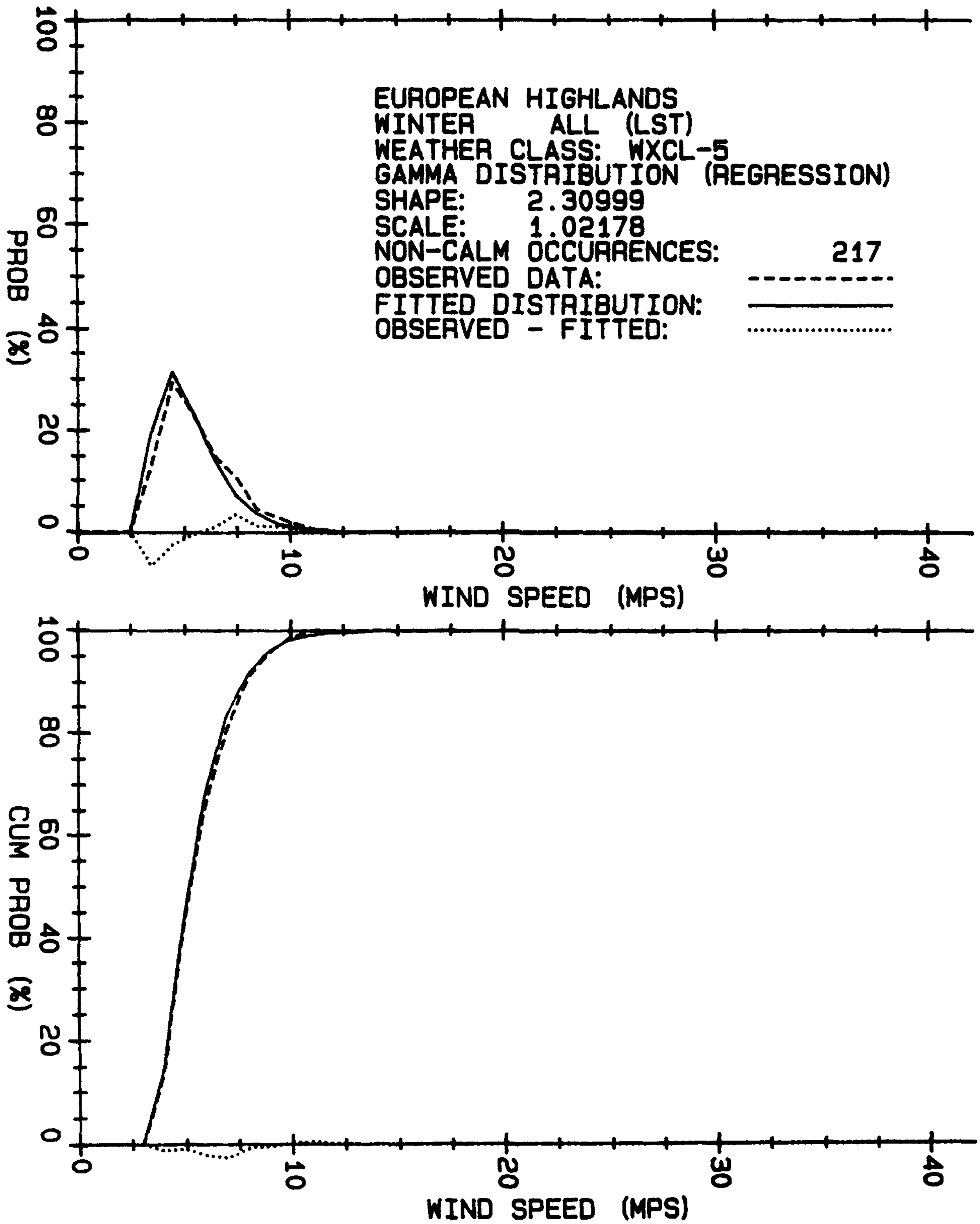

Figure 21. Regression fitted gamma distribution for European Highlands winter wind speeds for weather class 5.

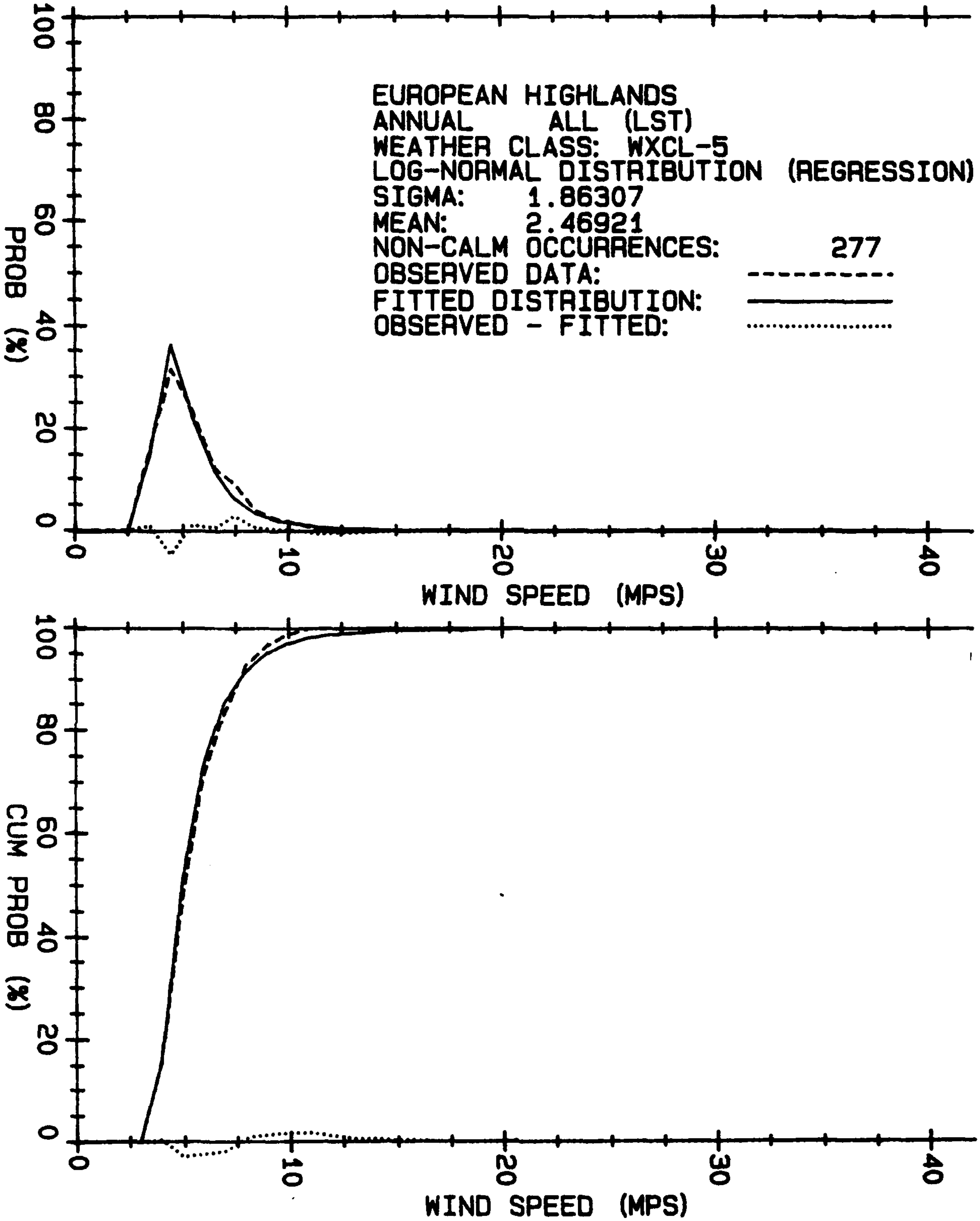

Figure 22. Regression fitted log-normal distribution for European Highlands wind speeds for weather class 5.

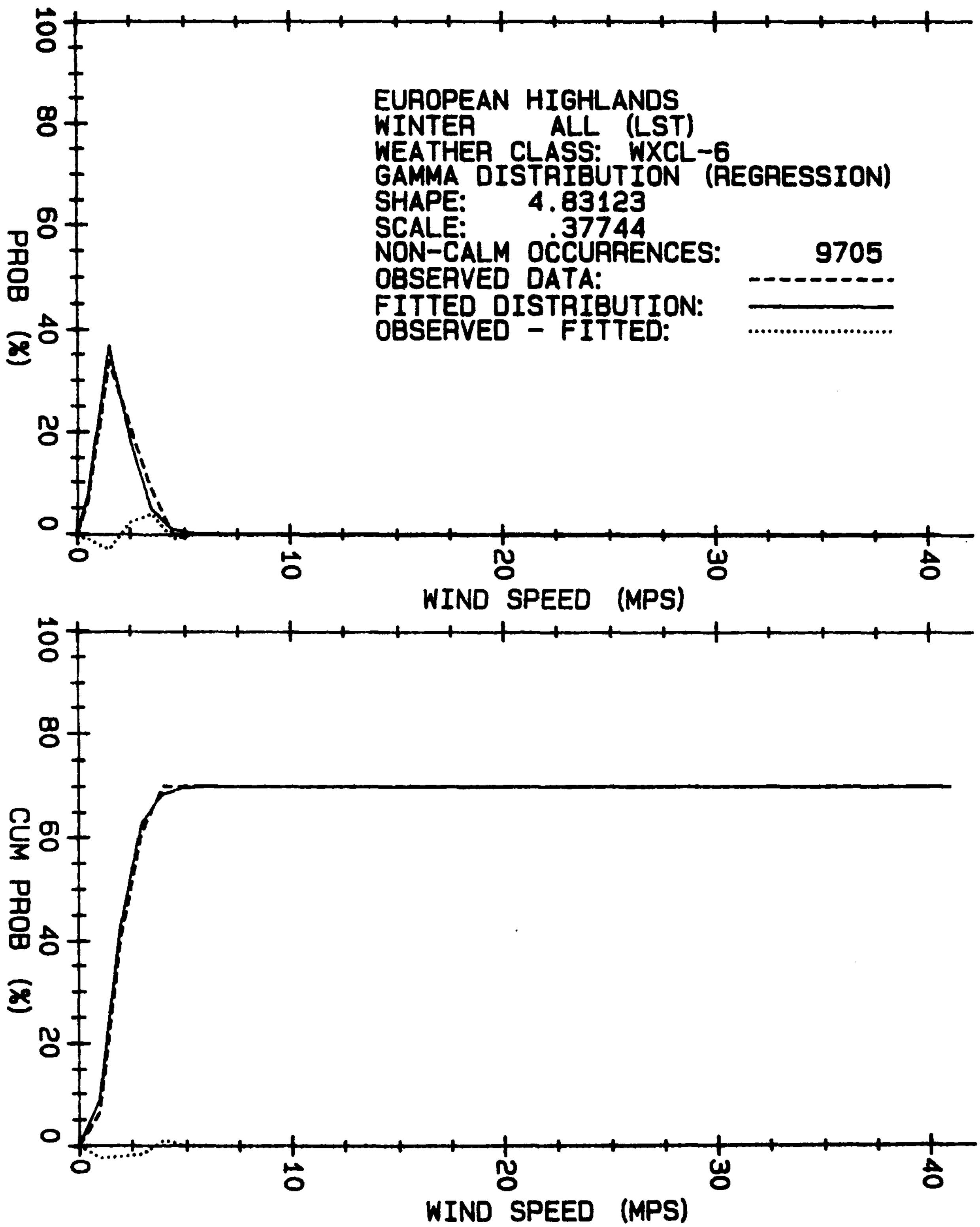

Figure 23. Regression fitted gamma distribution for European Highlands winter wind speeds for weather class 6.

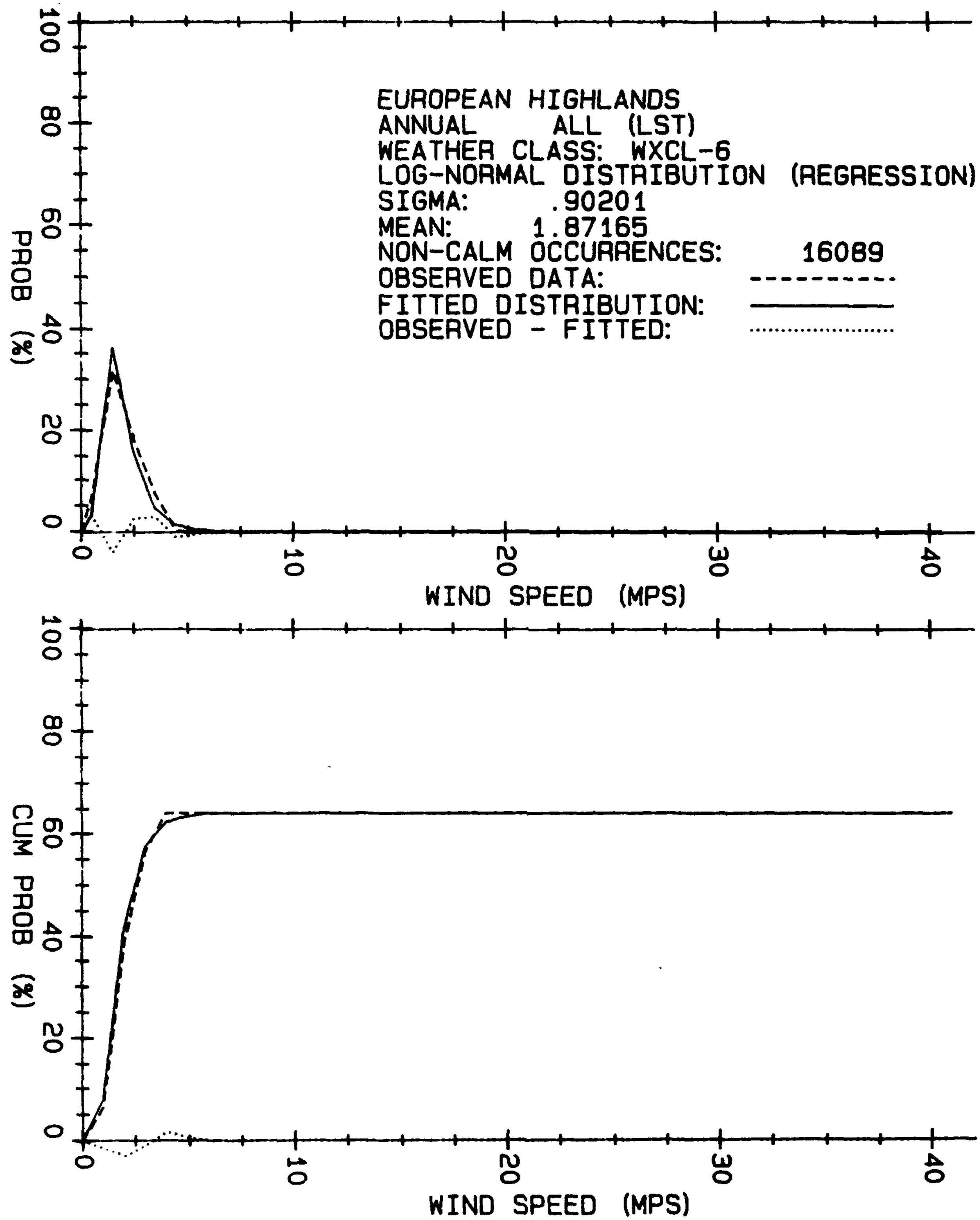

Figure 24. Regression fitted log-normal distribution for European Highlands wind speeds for weather class 6.

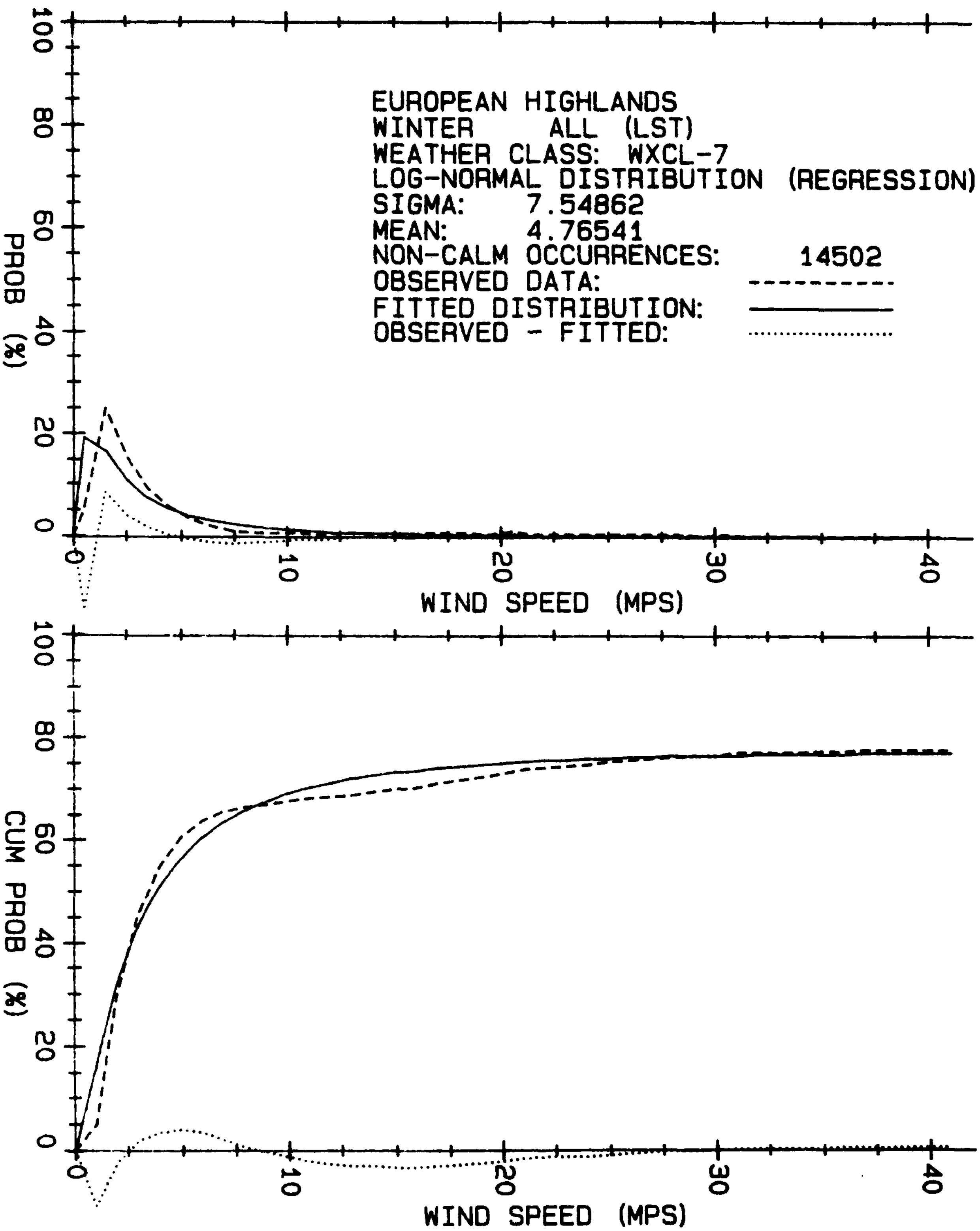

Figure 25. Regression fitted log-normal distribution for European Highlands winter wind speeds for weather class 7.

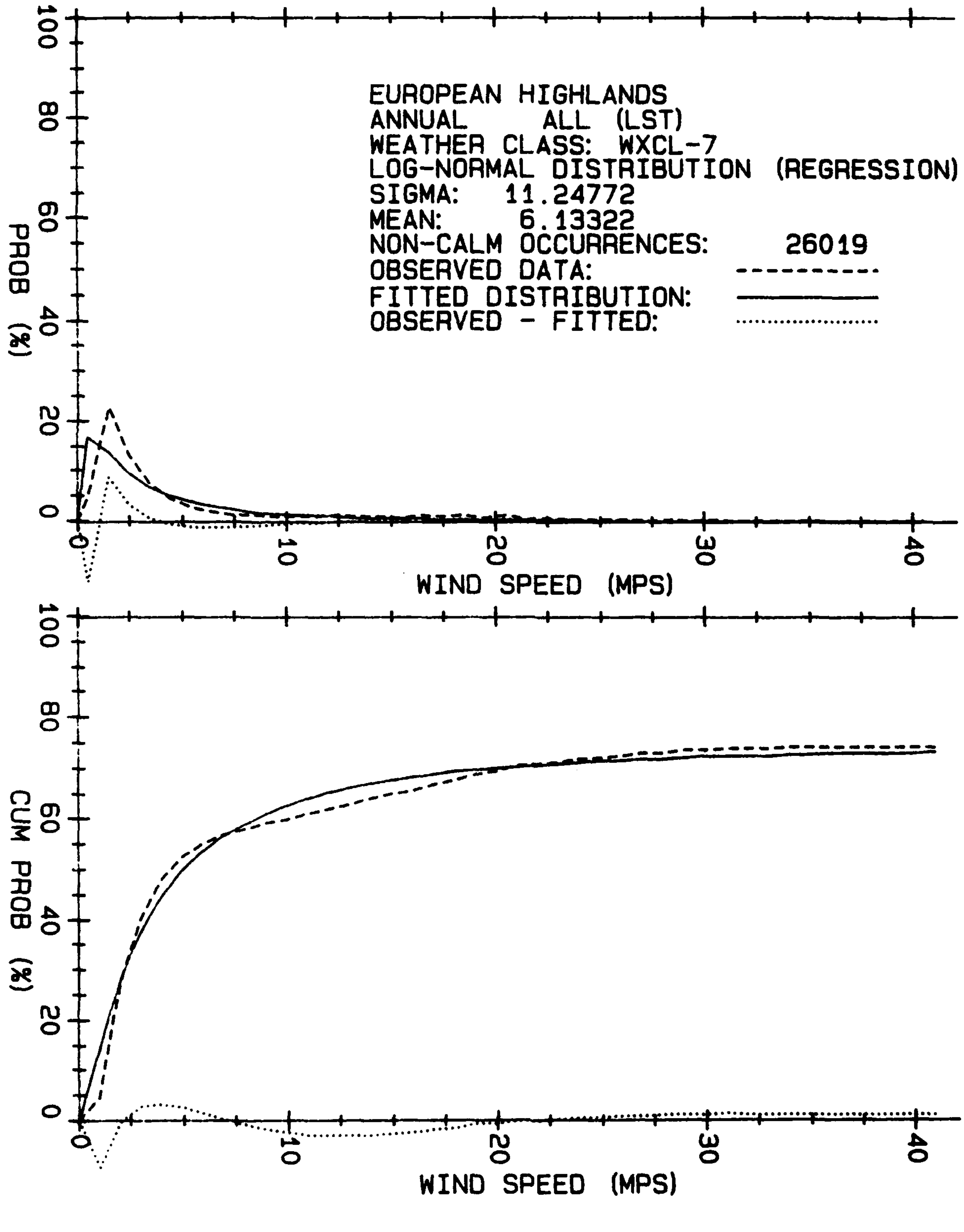

Figure 26. Regression fitted log-normal distribution for European Highlands wind speeds for weather class 7.

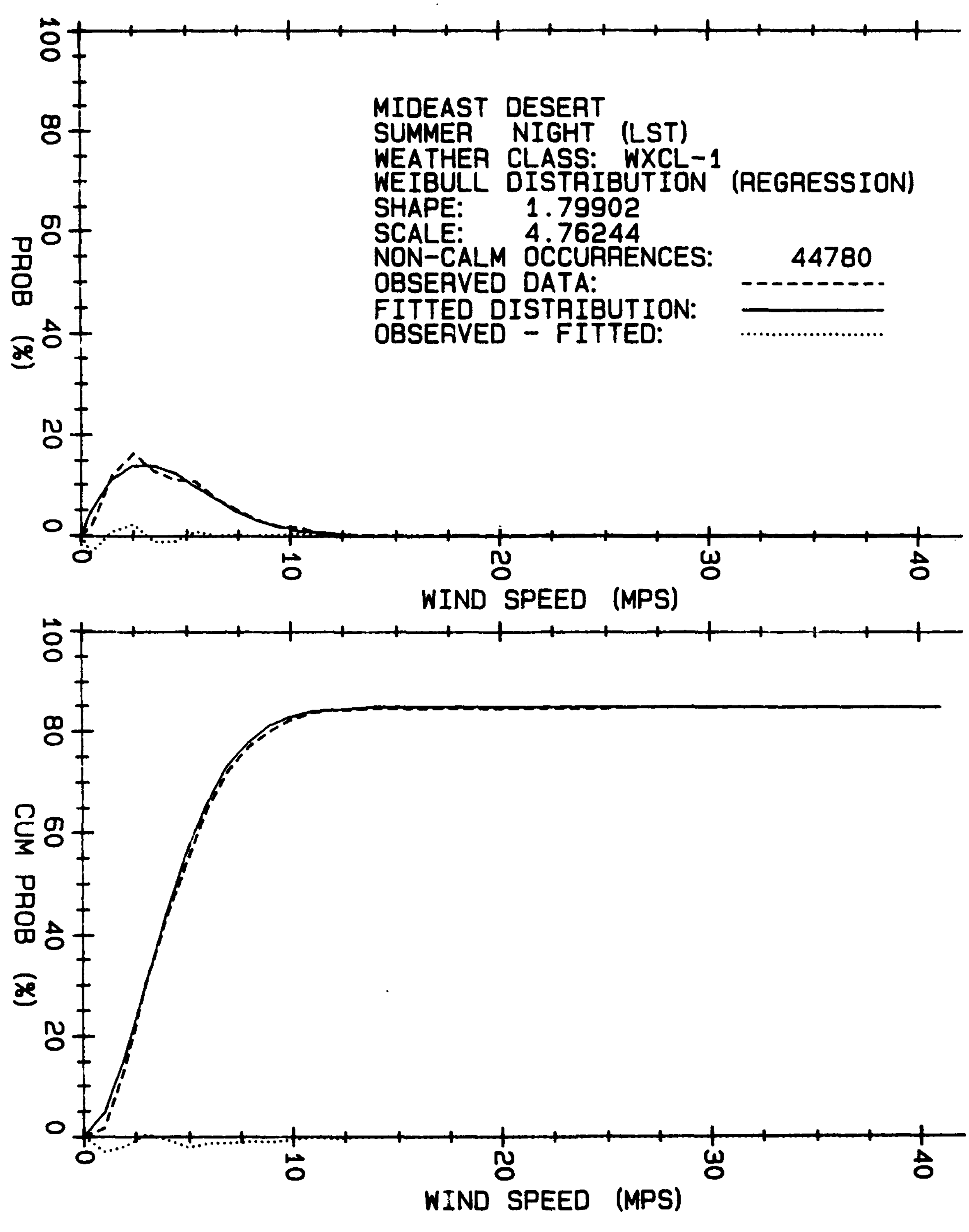

Figure 27. Regression fitted Weibull distribution for Mideast Desert night-time summer wind speeds for weather class 1.

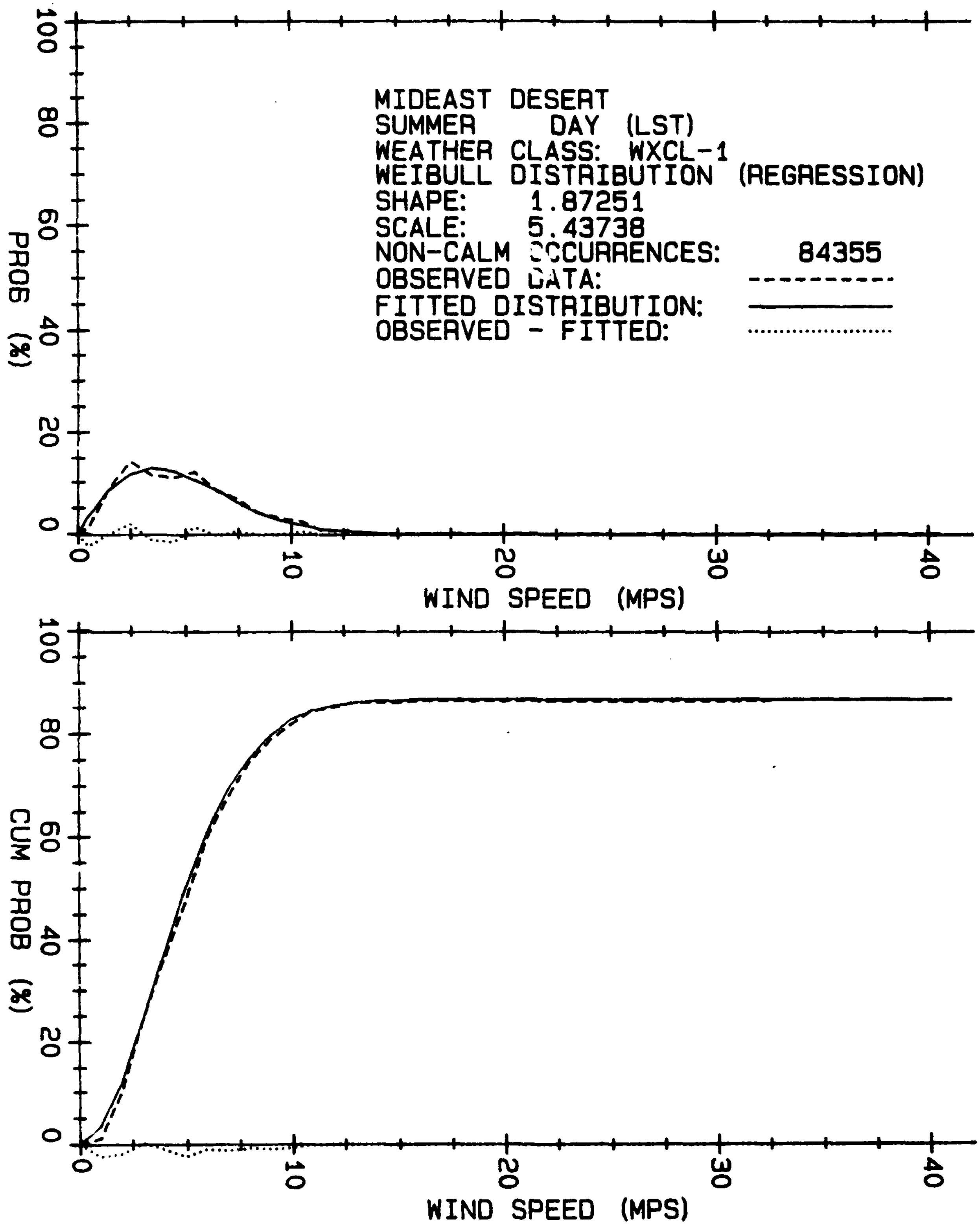

Figure 28. Regression fitted Weibull distribution for Mideast Desert day-time summer wind speeds for weather class 1.

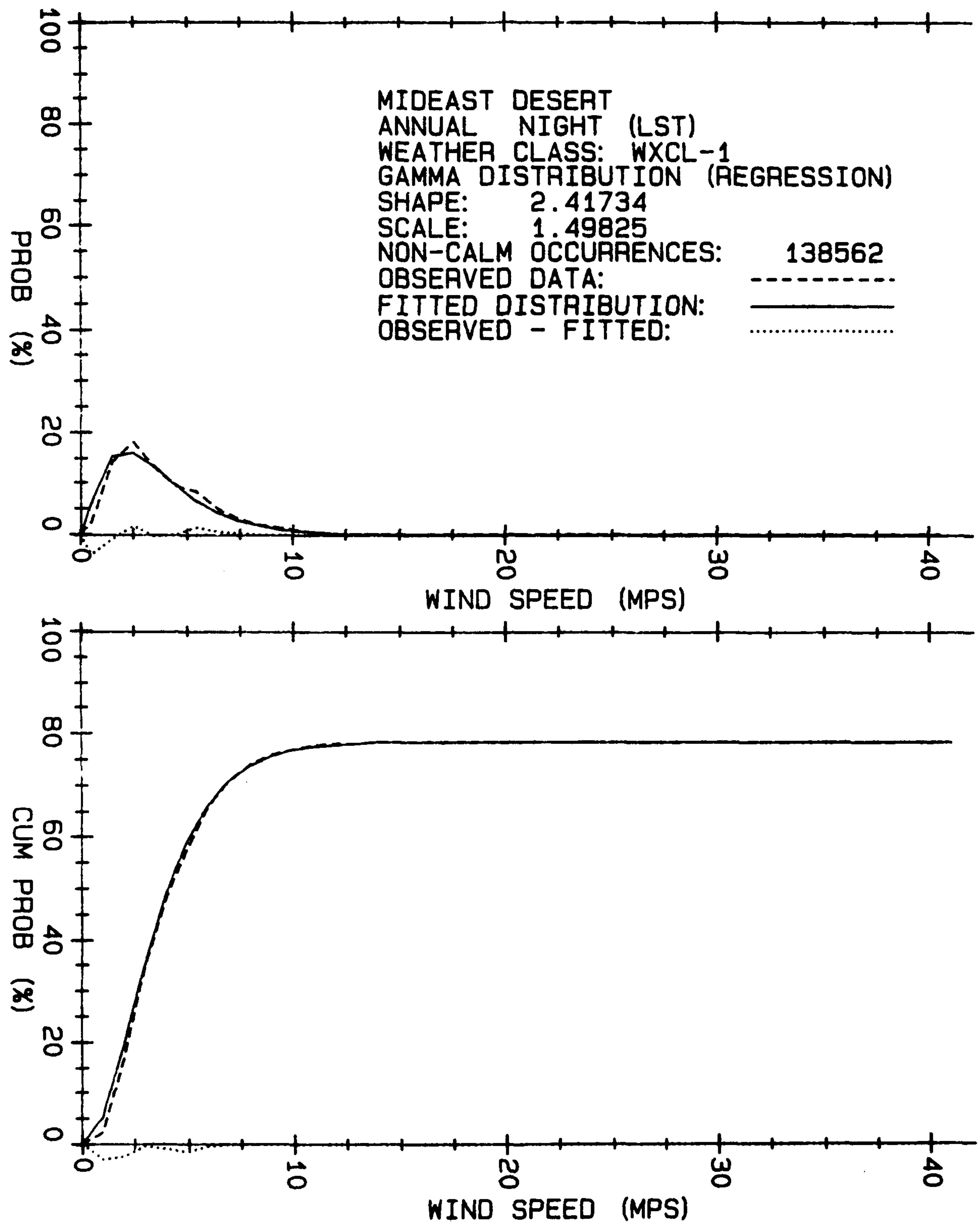

Figure 29. Regression fitted gamma distribution for Mideast Desert nighttime wind speeds for weather class 1.

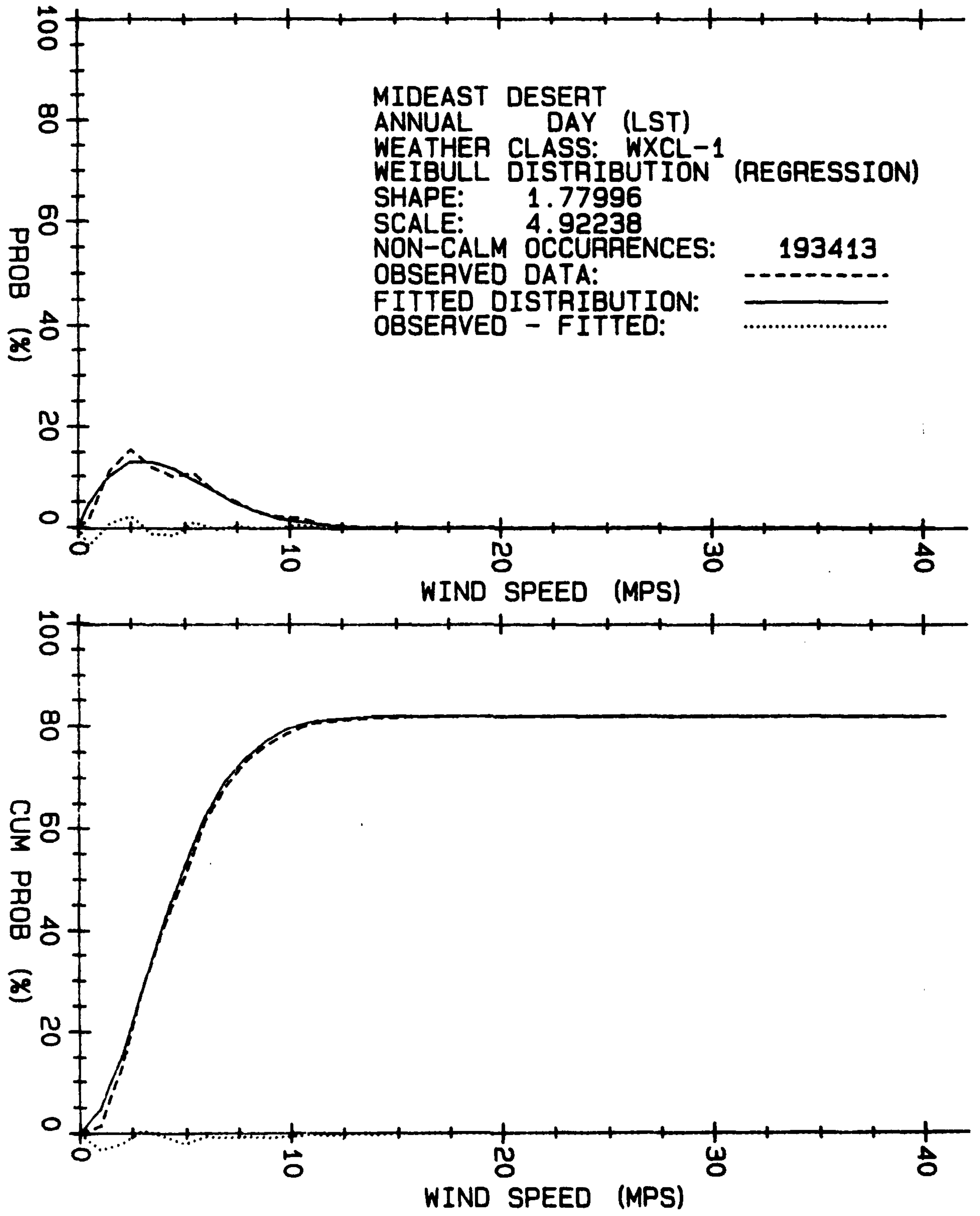

Figure 30. Regression fitted Weibull distribution for Mideast Desert daytime wind speeds for weather class 1.

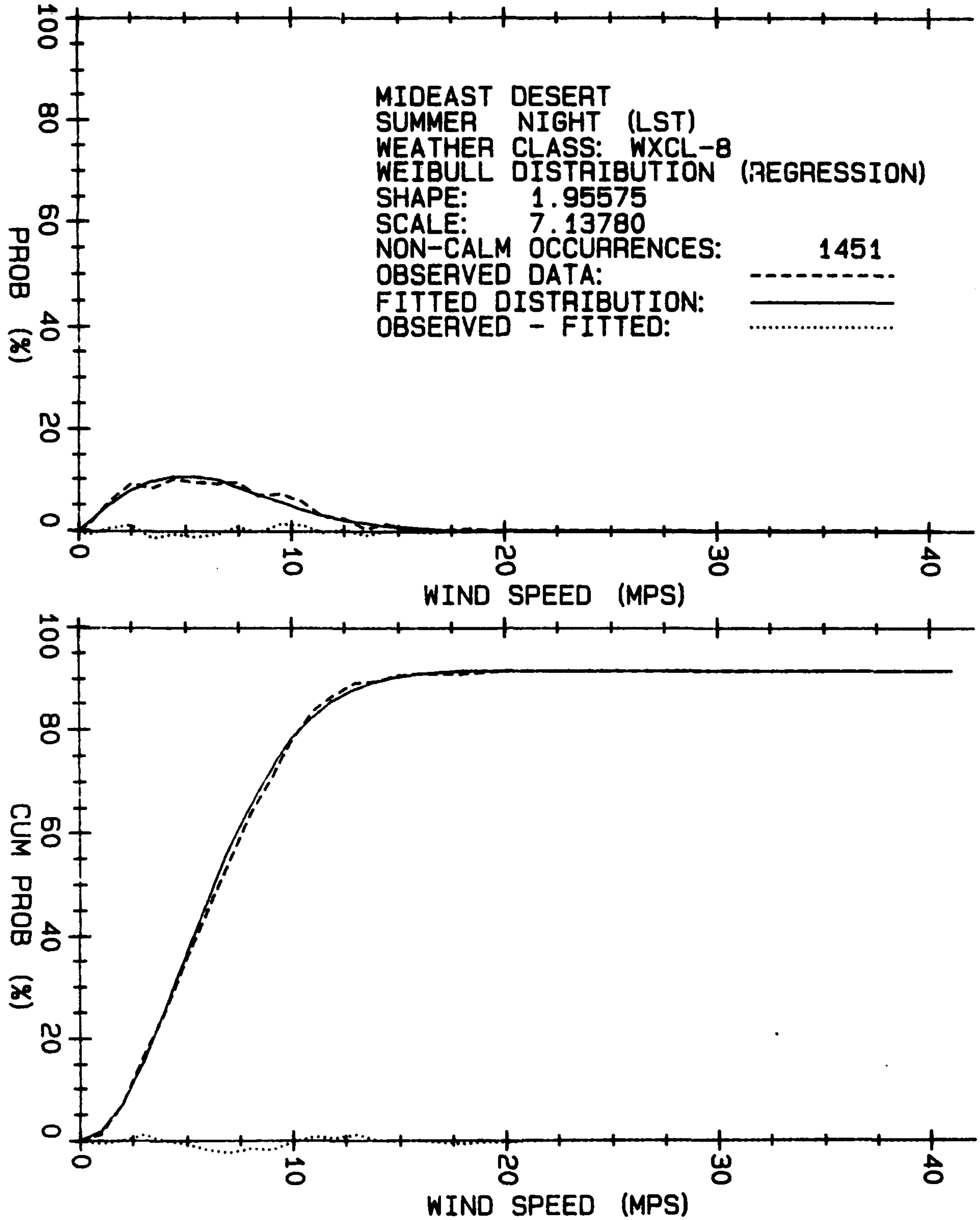

Figure 31. Regression fitted Weibull distribution for Mideast Desert nighttime summer wind speeds for weather class 8.

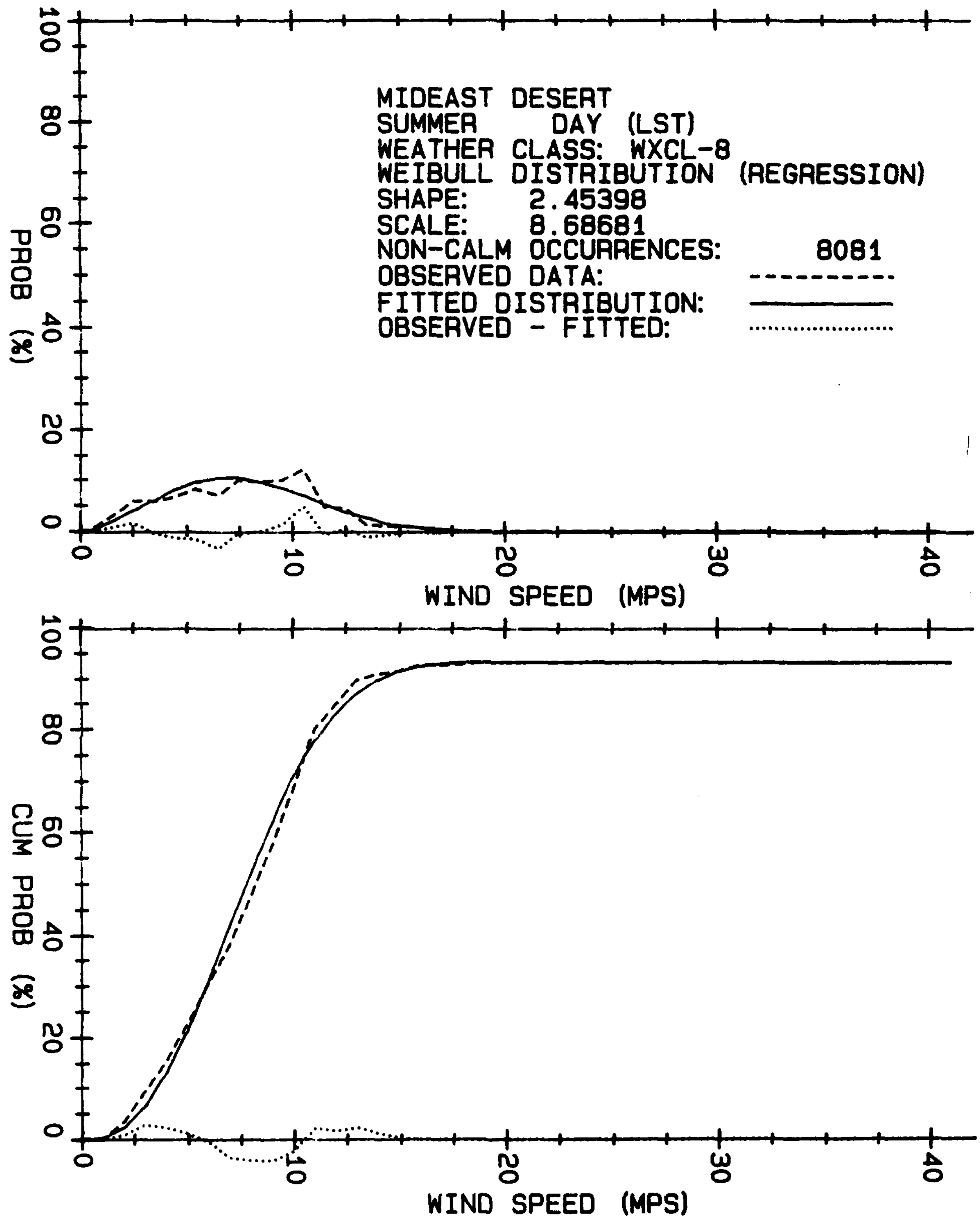

Figure 32. Regression fitted Weibull distribution for Mideast Desert daytime summer wind speeds for weather class 8.

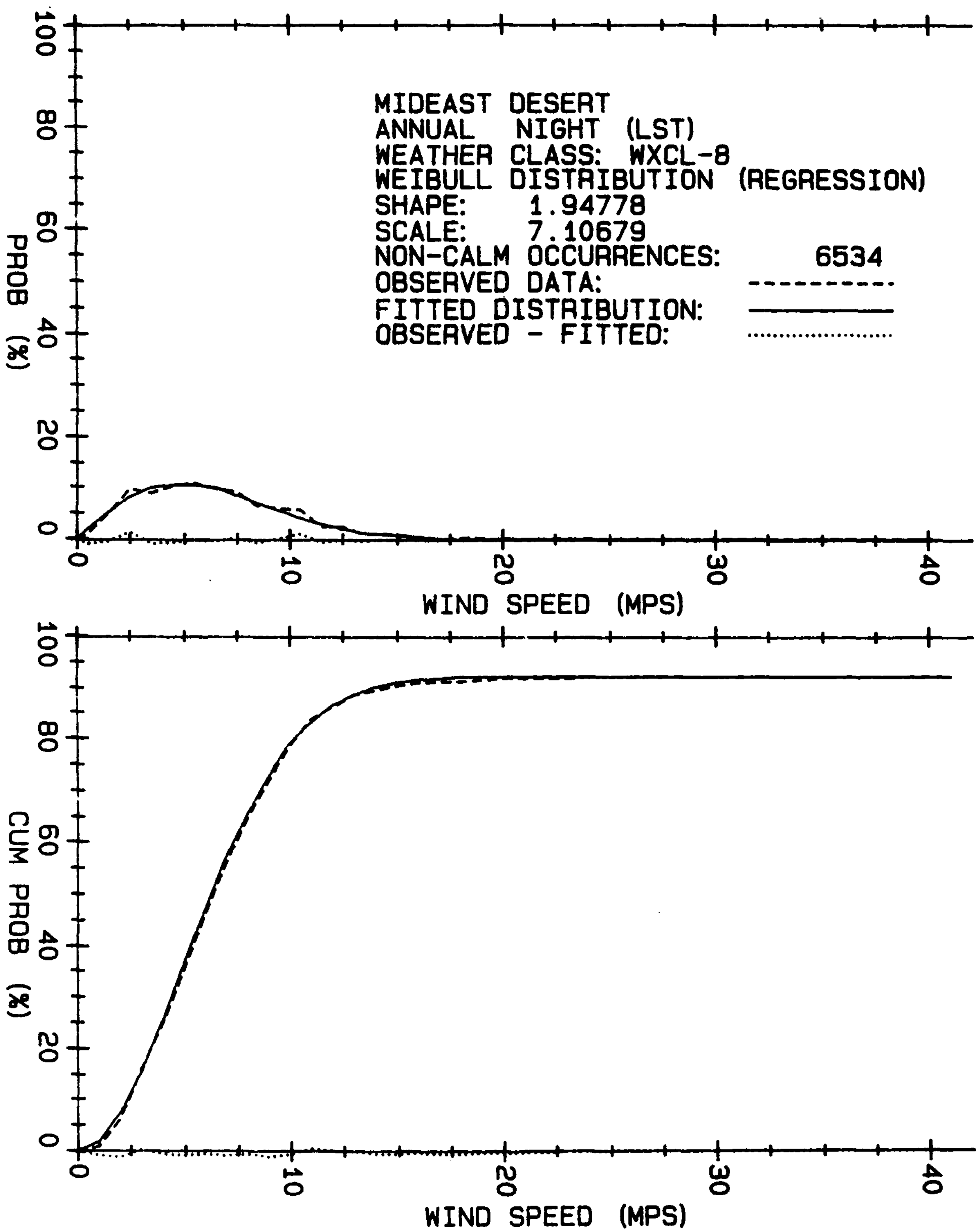

Figure 33. Regression fitted Weibull distribution for Mideast Desert night-time wind speeds for weather class 8.

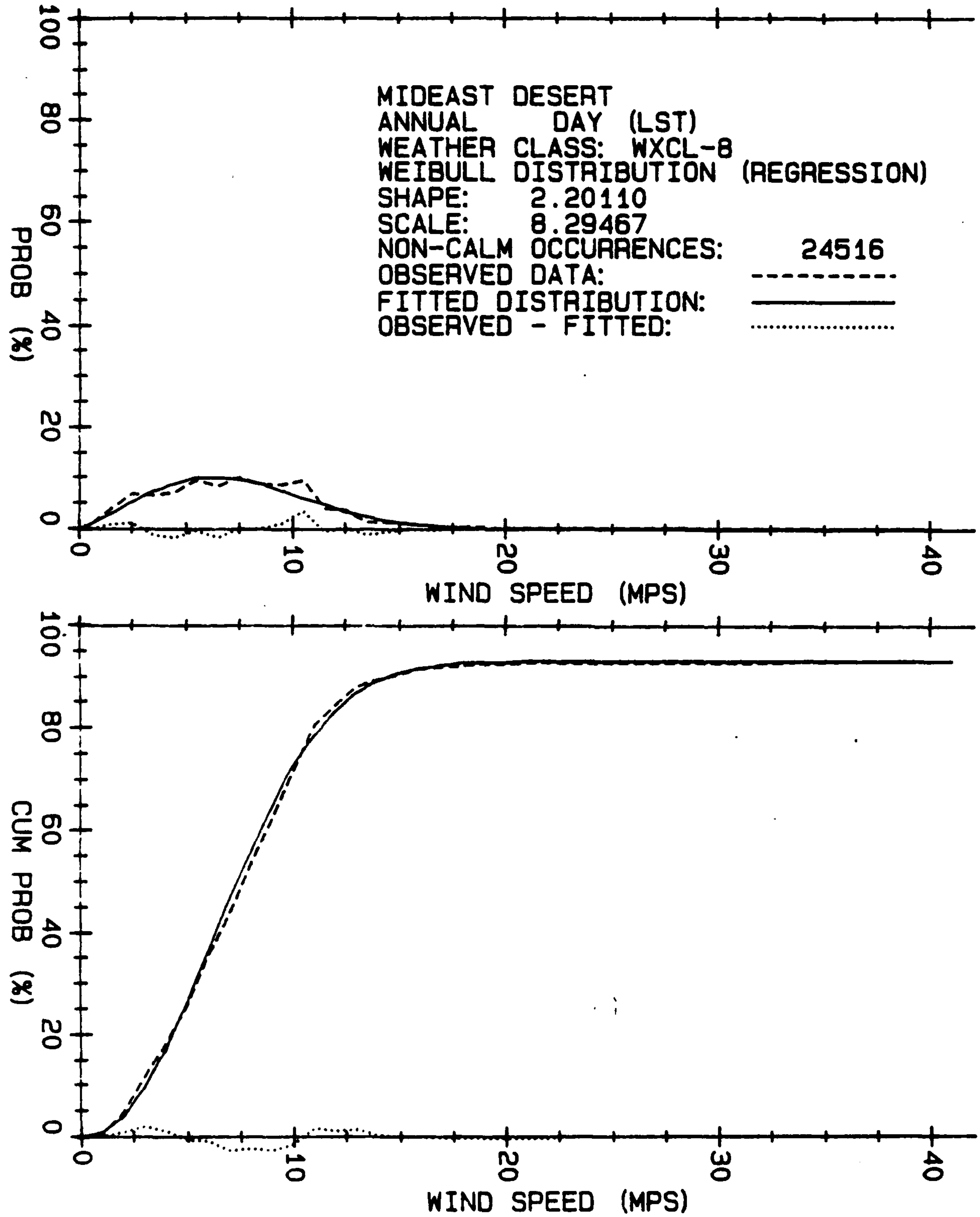

Figure 34. Regression fitted Weibull distribution for Mideast Desert daytime wind speeds for weather class 8.

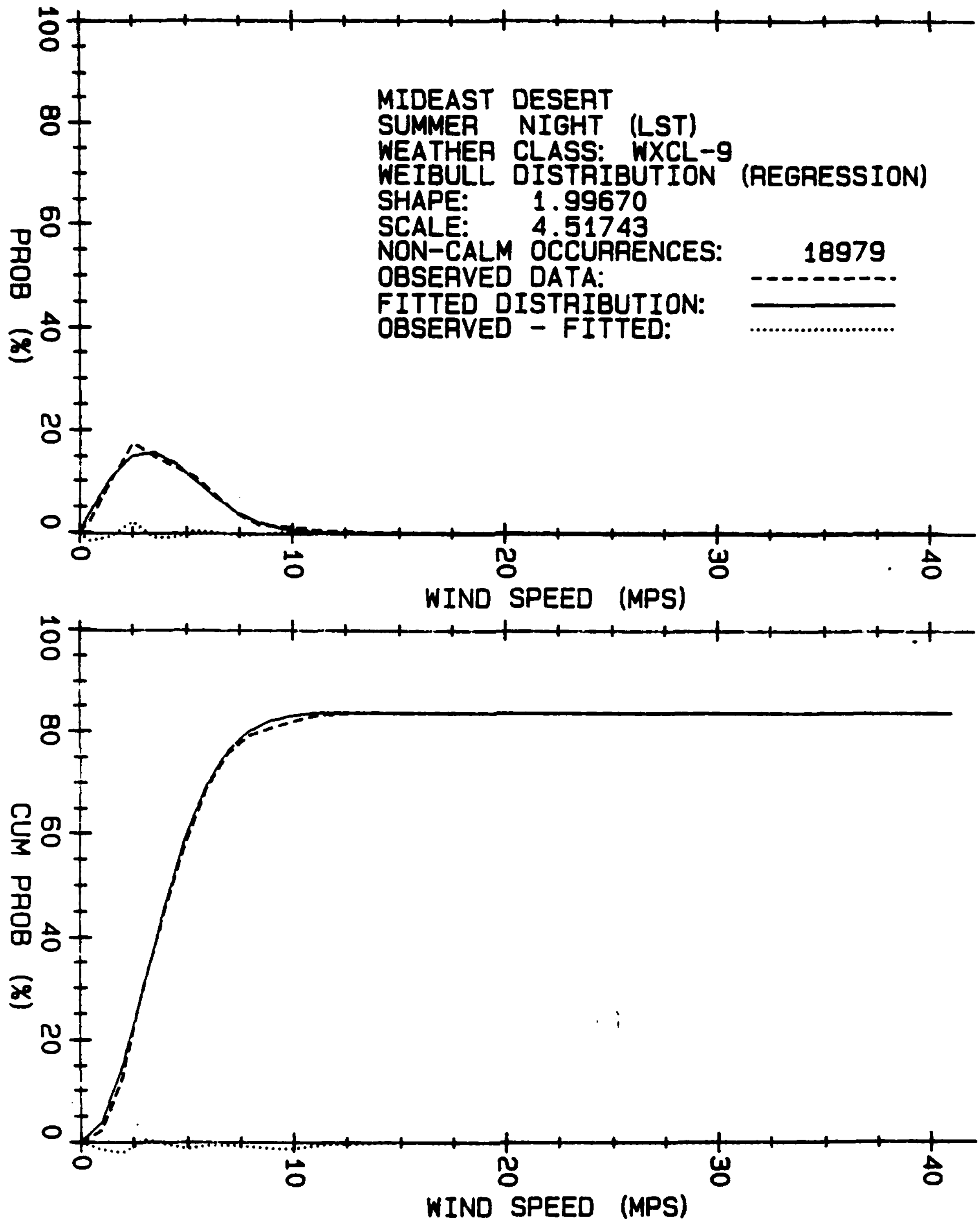

Figure 35. Regression fitted Weibull distribution for Mideast Desert night-time summer wind speeds for weather class 9.

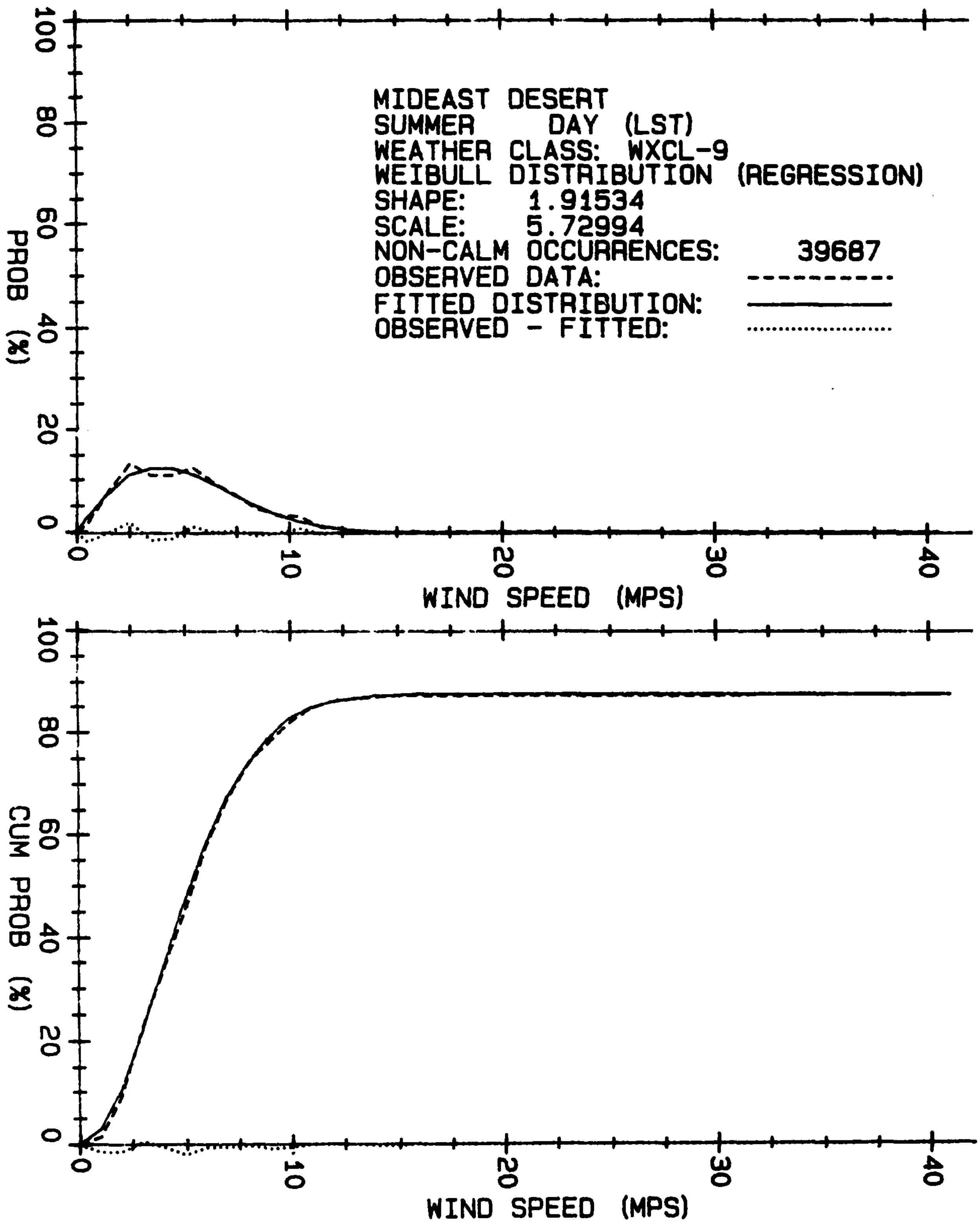

Figure 36. Regression fitted Weibull distribution for Mideast Desert daytime summer wind speeds for weather class 9.

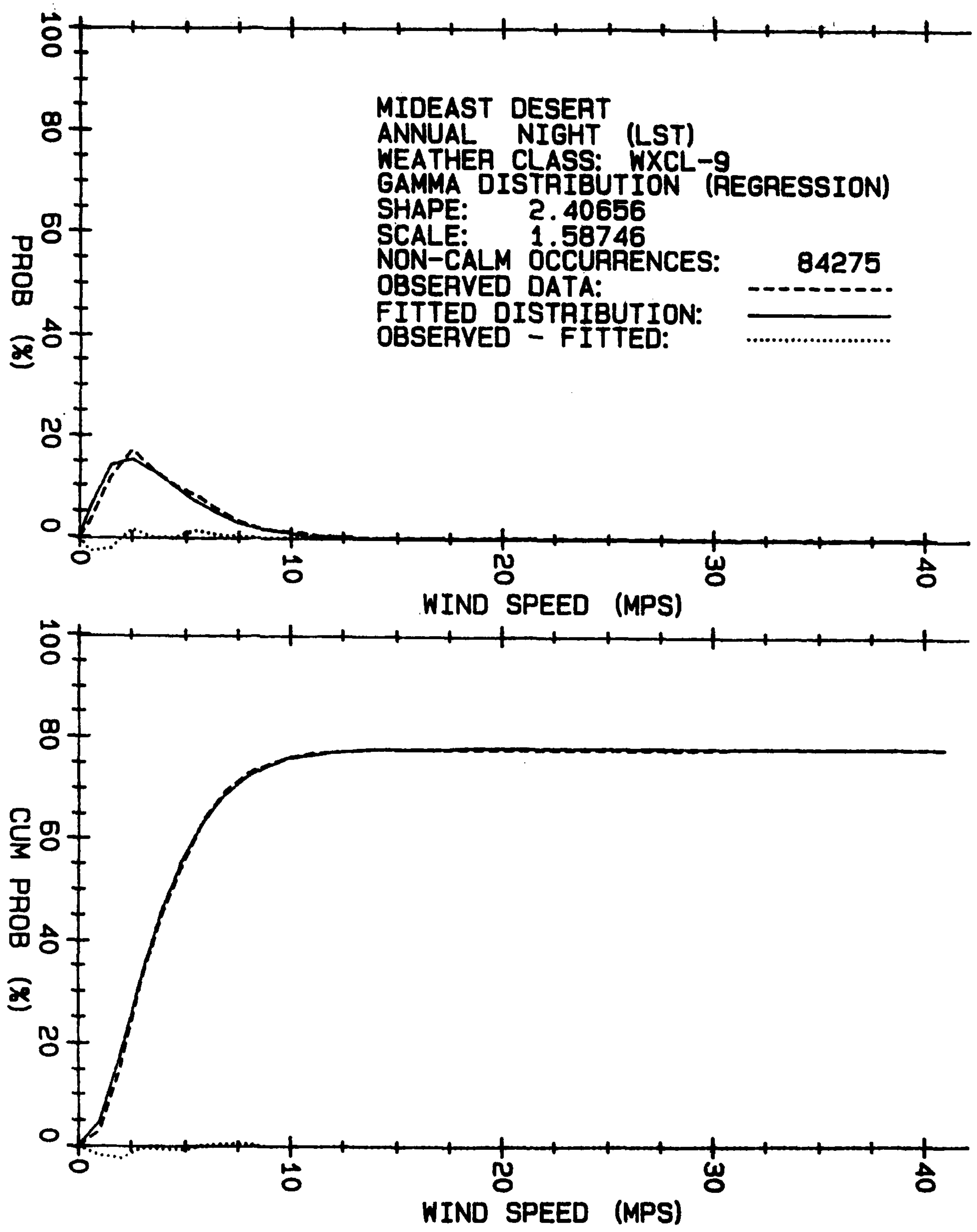

Figure 37. Regression fitted gamma distribution for Mideast Desert nighttime wind speeds for weather class 9.

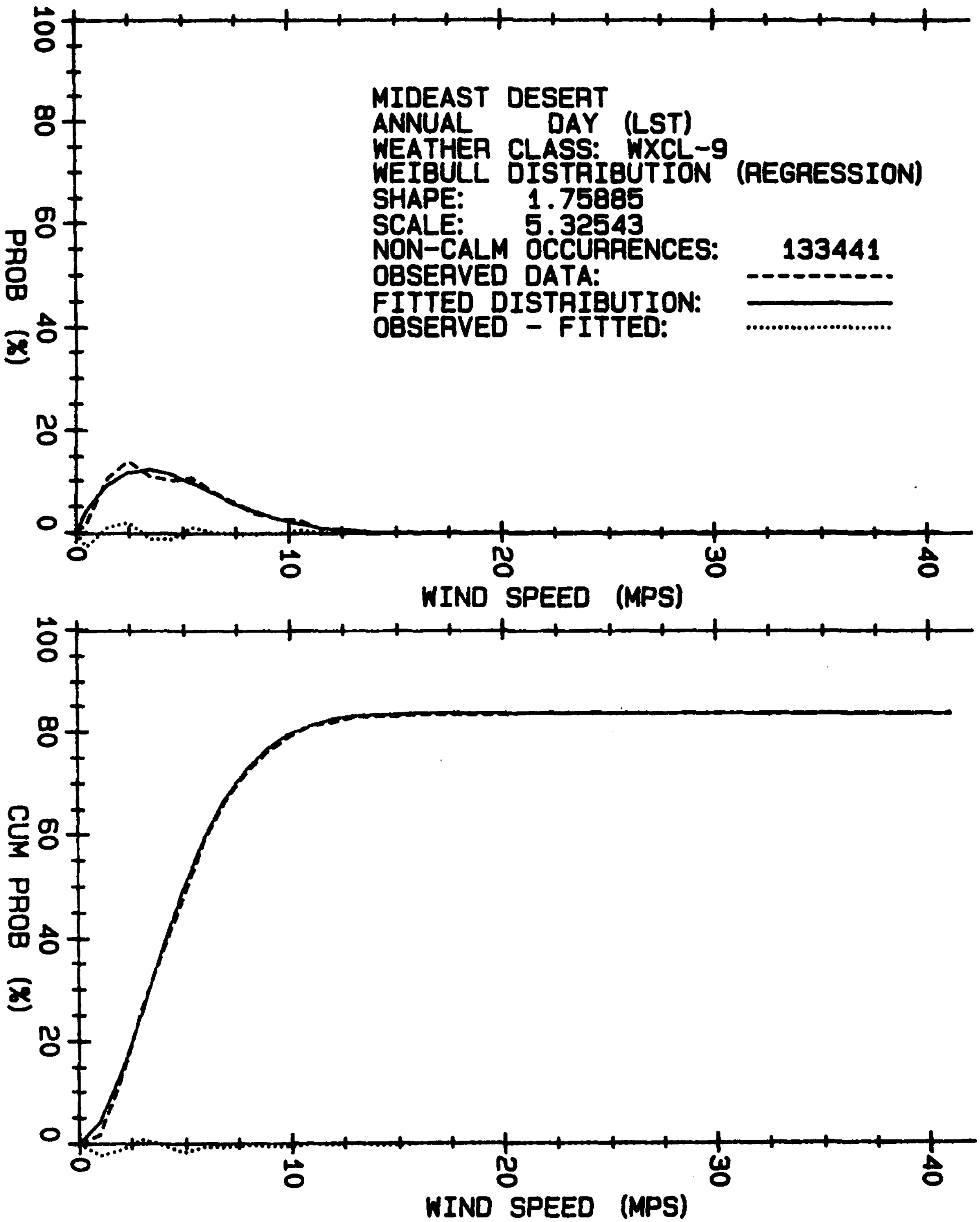

Figure 38. Regression fitted Weibull distribution for Mideast Desert daytime wind speeds for weather class 9.

LITERATURE CITED

Baynes, C. J., 1974, The statistics of strong winds for engineering applications, Res. Rpt. BLWT-4-1974, Engineering Science Dept., U. Western Ontario, Canada, 265 pp.

Baynes, C. J., and A. G. Davenport, 1975, "Some statistical models for wind climate prediction," Preprints 4th Conference Probability and Statistics in the Atmospheric Sciences, Tallahassee, Florida, American Meteorological Society, Boston, MA, pp. 1-7.

Crutcher, H. L., and L. Baer, 1962, "Computations from elliptical wind distribution statistics," J Appl Meteorol, 14:1512-1520.

Dinkelacker, O., 1949, "Uber spezielle windverteilungfunktionen," Wetter Klima, 2:129-138.

Hennessey, J. P., 1977, "Some Aspects of Wind Power Statistics," J Appl Meteorol, 16:119-128.

Holton, J. R., 1967, "The diurnal boundary layer wind oscillation above sloping terrain," Tellus, 19:199-205.

Justus, C. G., W. R. Hargraves, and A. Yalcin, 1976, "Nationwide assessment of potential output from wind powered generators," J Appl Meteorol, 15:673-678.

Luna, R. E., and H. W. Church, 1974, "Estimation of long-term concentrations using a 'universal' wind speed distribution," J Appl Meteorol, 13:910-916.

Mage, D. T., 1980, "Frequency distributions of hourly wind speed measurements," Atmospheric Environment, 14:367-374.

Miers, Bruce T., Elton P. Avara, and Louis D. Duncan, 1985a, Global Electro-Optical Systems Environmental Matrix (GEOSEM) Climatology for Mideast and Southwest Asia, ASL-TR-0172, U.S. Army Atmospheric Sciences Laboratory, White Sands Missile Range, NM 88002-5501.

Miers, Bruce T., Elton P. Avara, and Louis D. Duncan, 1985b, Global Electro-Optical Systems Environmental Matrix (GEOSEM) Climatology for Central and Northern Europe, ASL-TR-0177, U.S. Army Atmospheric Sciences Laboratory, White Sands Missile Range, NM 88002-5501.

Narovlyanskii, G. Y., 1968, "Aviation Climatology," TT-69-55100, National Technical Information Service, Atlanta, Georgia.

Putnam, P. C., 1948, Power from the Wind, Von Nostrand Publications, 224 pp.

Sherlock, R. H., 1951, "Analyzing winds for frequency and duration," Meteorol Monogr, 4:72-79., American Meteorological Society, Boston, MA.

Stewart, D. A., and O. M. Essenwanger, 1978, "Frequency distributions of wind speed near the surface," J Appl Meteorol, 17:1633-1642.

U.S. Air Force Environmental Technical Applications Center (USAFETAC), 1991, EO Climatology Version 2.0 Microcomputer Program, U.S. Air Force Environmental Technical Applications Center, Scott Air Force Base, IL 62225-5438.

Wentink, T., 1974, "Wind power potential of Alaska; Part I," PB 238-507, National Technical Information Service, Atlanta, Georgia.

Wentink, T., 1976, "Study of Alaskan wind power and its possible applications," PB 253-339, National Technical Information Services, Atlanta, Georgia.

DISTRIBUTION LIST FOR PUBLIC RELEASE

Commandant
U.S. Army Chemical School
ATTN: ATZN-CM-CC (S. Barnes)
Fort McClellan, AL 36205-5020

Commander
U.S. Army Aviation Center
ATTN: ATZQ-D-MA
Mr. Oliver N. Heath
Fort Rucker, AL 36362

Commander
U.S. Army Aviation Center
ATTN: ATZQ-D-MS (Mr. Donald Wagner)
Fort Rucker, AL 36362

NASA/Marshall Space Flight Center
Deputy Director
Space Science Laboratory
Atmospheric Sciences Division
ATTN: E501 (Dr. George H. Fichtl)
Huntsville, AL 35802

NASA/Marshall Space Flight Center
Atmospheric Sciences Division
ATTN: Code ED-41
Huntsville, AL 35812

Deputy Commander
U.S. Army Strategic Defense Command
ATTN: CSSD-SL-L
Dr. Julius Q. Lilly
P.O. Box 1500
Huntsville, AL 35807-3801

Commander
U.S. Army Missile Command
ATTN: AMSMI-RD-AC-AD
Donald R. Peterson
Redstone Arsenal, AL 35898-5242

Commander
U.S. Army Missile Command
ATTN: AMSMI-RD-AS-SS
Huey F. Anderson
Redstone Arsenal, AL 35898-5253

Commander
U.S. Army Missile Command
ATTN: AMSMI-RD-AS-SS
B. Williams
Redstone Arsenal, AL 35898-5253

Commander
U.S. Army Missile Command
ATTN: AMSMI-RD-DE-SE
Gordon Lill, Jr.
Redstone Arsenal, AL 35898-5245

Commander
U.S. Army Missile Command
Redstone Scientific Information Center
ATTN: AMSMI-RD-CS-R/Documents
Redstone, Arsenal, AL 35898-5241

Commander
U.S. Army Intelligence Center and Fort Huachuca
ATTN: ATSI-CDC-C (Mr. Colanto)
Fort Huachuca, AZ 85613-7000

Northrup Corporation
Electronics Systems Division
ATTN: Dr. Richard D. Tooley
2301 West 120th Street, Box 5032
Hawthorne, CA 90251-5032

Commander - Code 3331
Naval Weapons Center
ATTN: Dr. Alexis Shlanta
China Lake, CA 93555

Commander
Pacific Missile Test Center
Geophysics Division
ATTN: Code 3250 (Terry E. Battalino)
Point Mugu, CA 93042-5000

Lockheed Missiles & Space Co., Inc.
Kenneth R. Hardy
Org/91-01 B/255
3251 Hanover Street
Palo Alto, CA 94304-1191

Commander
Naval Ocean Systems Center
ATTN: Code 54 (Dr. Juergen Richter)
San Diego, CA 92152-5000

Meteorologist in Charge
Kwajalein Missile Range
P.O. Box 67
APO San Francisco, CA 96555

U.S. Department of Commerce
Mountain Administration Support
Center
Library, R-51 Technical Reports
325 S. Broadway
Boulder, CO 80303

Dr. Hans J. Liebe
NTIA/ITS S 3
325 S. Broadway
Boulder, CO 80303

NCAR Library Serials
National Center for Atmos Rsch
P.O. Box 3000
Boulder, CO 80307-3000

HQDA
ATTN: DAMI-POI
Washington, D.C. 20310-1067

Mil Asst for Env Sci Ofc of
The Undersecretary of Defense
for Rsch & Engr/R&AT/E&LS
Pentagon - Room 3D129
Washington, D.C. 20301-3080

Director
Naval Research Laboratory
ATTN: Code 4110
Dr. Lothar H. Ruhnke
Washington, D.C. 20375-5000

HQDA
DEAN-RMD/Dr. Gomez
Washington, D.C. 20314

Director
Division of Atmospheric Science
National Science Foundation
ATTN: Dr. Eugene W. Bierly
1800 G. Street, N.W.
Washington, D.C. 20550

Commander
Space & Naval Warfare System Command
ATTN: PMW-145-1G (LT Painter)
Washington, D.C. 20362-5100

Commandant
U.S. Army Infantry
ATTN: ATSH-CD-CS-OR
Dr. E. Dutoit
Fort Benning, GA 30905-5090

USAFETAC/DNE
Scott AFB, IL 62225

Air Weather Service
Technical Library - FL4414
Scott AFB, IL 62225-5458

HQ AWS/DOO
Scott AFB, IL 62225-5008

USAFETAC/DNE
ATTN: Mr. Charles Glauber
Scott AFB, IL 62225-5008

Commander
U.S. Army Combined Arms Combat
ATTN: ATZL-CAW (LTC A. Kyle)
Fort Leavenworth, KS 66027-5300

Commander
U.S. Army Combined Arms Combat
ATTN: ATZL-CDB-A (Mr. Annett)
Fort Leavenworth, KS 66027-5300

Commander
U.S. Army Space Institute
ATTN: ATZI-SI (Maj Koepsell)
Fort Leavenworth, KS 66027-5300

Commander
U.S. Army Space Institute
ATTN: ATZL-SI-D
Fort Leavenworth, KS 66027-7300

Commander
Phillips Lab
ATTN: PL/LYP (Mr. Chisholm)
Hanscom AFB, MA 01731-5000

Director
Atmospheric Sciences Division
Geophysics Directorate
Phillips Lab
ATTN: Dr. Robert A. McClatchey
Hanscom AFB, MA 01731-5000

Raytheon Company
Dr. Charles M. Sonnenschein
Equipment Division
528 Boston Post Road
Sudbury, MA 01776
Mail Stop 1K9

Director
U.S. Army Materiel Systems
Analysis Activity
ATTN: AMXSY-MP (H. Cohen)
APG, MD 21005-5071

Commander
U.S. Army Chemical Rsch,
Dev & Engr Center
ATTN: SMCCR-OPA (Ronald Pennsyle)
APG, MD 21010-5423

Commander
U.S. Army Chemical Rsch,
Dev & Engr Center
ATTN: SMCCR-RS (Mr. Joseph Vervier)
APG, MD 21010-5423

Commander
U.S. Army Chemical Rsch,
Dev & Engr Center
ATTN: SMCCR-MUC (Mr. A. Van De Wal)
APG, MD 21010-5423

Director
U.S. Army Materiel Systems
Analysis Activity
ATTN: AMXSY-AT (Mr. Fred Campbell)
APG, MD 21005-5071

Director
U.S. Army Materiel Systems
Analysis Activity
ATTN: AMXSY-CR (Robert N. Marchetti)
APG, MD 21005-5071

Director
U.S. Army Materiel Systems
Analysis Activity
ATTN: AMXSY-CS (Mr. Brad W. Bradley)
APG, MD 21005-5071

Commander
U.S. Army Laboratory Command
ATTN: AMSLC-CG
2800 Powder Mill Road
Adelphi, MD 20783-1145

Commander
Headquarters
U.S. Army Laboratory Command
ATTN: AMSLC-CT
2800 Powder Mill Road
Adelphi, MD 20783-1145

Commander
Harry Diamond Laboratories
ATTN: SLCIS-CO
2800 Powder Mill Road
Adelphi, MD 20783-1197

Director
Harry Diamond Laboratories
ATTN: SLCHD-ST-SP
Dr. Z.G. Sztankay
Adelphi, MD 20783-1197

National Security Agency
ATTN: W21 (Dr. Longbothum)
9800 Savage Road
Ft George G. Meade, MD 20755-6000

U. S. Army Space Technology
and Research Office
ATTN: Brenda Brathwaite
5321 Riggs Road
Gaithersburg, MD 20882

OIC-NAVSWC
Technical Library (Code E-232)
Silver Springs, MD 20903-5000

The Environmental Research
Institute of MI
ATTN: IRIA Library
P.O. Box 8618
Ann Arbor, MI 48107-8618

Commander
U.S. Army Research Office
ATTN: DRXRO-GS (Dr. W.A. Flood)
P.O. Box 12211
Research Trianagle Park, NC 27709

Dr. Jerry Davis
North Carolina State University
Department of Marine, Earth, &
Atmospheric Sciences
P.O. Box 8208
Raleigh, NC 27650-8208

Commander
U. S. Army CECRL
ATTN: CECRL-RG (Dr. H. S. Boyne)
Hanover, NH 03755-1290

Commanding Officer
U.S. Army ARDEC
ATTN: SMCAR-IMI-I, Bldg 59
Dover, NJ 07806-5000

U.S. Army Communications-Electronics
Command Center for EW/RSTA
ATTN: AMSEL-RD-EW-SP
Fort Monmouth, NJ 07703-5303

Commander
U.S. Army Communications-Electronics
Command
ATTN: AMSEL-EW-D (File Copy)
Fort Monmouth, NJ 07703-5303

Headquarters
U.S. Army Communications-Electronics
Command
ATTN: AMSEL-EW-MD
Fort Monmouth, NJ 07703-5303

Commander
U.S. Army Satellite Comm Agency
ATTN: DRCPM-SC-3
Fort Monmouth, NJ 07703-5303

Director
EW/RSTA Center
ATTN: AMSEL-EW-DR
Fort Monmouth, NJ 07703-5303

USACECOM
Center for EW/RSTA
ATTN: AMSEL-RD-EW-SP
Fort Monmouth, NJ 07703-5303

6585th TG (AFSC)
ATTN: RX (CPT Stein)
Holloman AFB, NM 88330

Department of the Air Force
OL/A 2nd Weather Squadron (MAC)
Holloman AFB, NM 88330-5000

PL/WE
Kirtland AFB, NM 87118-6008

Director
U.S. Army TRADOC Analysis Command
ATTN: ATRC-WSS-R
White Sands Missile Range, NM 88002

Rome Laboratory
ATTN: Technical Library RL/DOVL
Griffiss AFB, NY 13441-5700

Department of the Air Force
7th Squadron
APO, NY 09403

AWS
USAREUR/AEAWX
APO, NY 09403-5000

AF Wright Aeronautical Laboratories
Avionics Laboratory
ATTN: AFWAL/AARI (Dr. V. Chimelis)
Wright-Patterson AFB, OH 45433

AFMC/DOW
Wright-Patterson AFB, OH 0334-5000

Commander
U.S. Army Field Artillery School
ATTN: ATSF-F-FD (Mr. Gullion)
Fort Sill, OK 73503-5600

Commandant
U.S. Army Field Artillery School
ATTN: ATSF-TSM-TA
Mr. Charles Taylor
Fort Sill, OK 73503-5600

Commander
Naval Air Development Center
ATTN: Al Salik (Code 5012)
Warminister, PA 18974

Commander
U.S. Army Dugway Proving Ground
ATTN: STEDP-MT-DA-M
Mr. Paul Carlson
Dugway, UT 84022

Commander
U.S. Army Dugway Proving Ground
ATTN: STEDP-MT-DA-L
Dugway, UT 84022

Commander
U.S. Army Dugway Proving Ground
ATTN: STEDP-MT-M (Mr. Bowers)
Dugway, UT 84022-5000

Defense Technical Information Center
ATTN: DTIC-FDAC
Cameron Station
Alexandria, VA 22314

Commanding Officer
U.S. Army Foreign Science &
Technology Center
ATTN: CM
220 7th Street, NE
Charlottesville, VA 22901-5396

Naval Surface Weapons Center
Code G63
Dahlgren, VA 22448-5000

Commander
U.S. Army OEC
ATTN: CSTE-EFS
Park Center IV
4501 Ford Ave
Alexandria, VA 22302-1458

Commander and Director
U.S. Army Corps of Engineers
Engineer Topographics Laboratory
ATTN: ETL-GS-LB
Fort Belvoir, VA 22060

TAC/DOWP
Langley AFB, VA 23665-5524

U.S. Army Topo Engineering Center
ATTN: CETEC-ZC
Fort Belvoir, VA 22060-5546

Commander
Logistics Center
ATTN: ATCL-CE
Fort Lee, VA 23801-6000

Commander
USATRADOC
ATTN: ATCD-FA
Fort Monroe, VA 23651-5170

Science and Technology
101 Research Drive
Hampton, VA 23666-1340

Commander
U.S. Army Nuclear & Chl Agency
ATTN: MONA-ZB Bldg 2073
Springfield, VA 22150-3198